



## SYNTHESIS OF NOVEL DERIVATIVES OF YAKUCHINONE B AS PROMISING ANTI-INFLAMMATORY AGENTS

Ajay Sehgal<sup>\*</sup>, Neha Sharma<sup>1</sup>, Pinki Phougat<sup>2</sup>, Ankita Sharma<sup>3</sup>, Shivani Pannu<sup>4</sup>, Rahul Pal<sup>5</sup>, Puja Gulati<sup>6</sup>, Dinesh Kumar<sup>7</sup>

<sup>\*</sup>Assistant Professor, School of Pharmaceutical Sciences, Om Sterling Global University, Hisar

<sup>1</sup>Assistant Professor, Department of Pharmaceutical Education and Research, Bhagat Phool Singh Mahila Vishwavidyalaya, Khanpur Kalan, Sonipat, Haryana

<sup>2</sup>Assistant Professor, Department of Pharmaceutical Education and Research, Bhagat Phool Singh Mahila Vishwavidyalaya, Khanpur Kalan, Sonipat, Haryana

<sup>3</sup>Assistant Professor, School of Pharmaceutical Sciences, Starex University, Gurugram, Haryana-122413

<sup>4</sup>Assistant Professor, School of Pharmacy, Desh Bhagat University, Mandi Gobindgarh, Punjab

<sup>5</sup>Assistant Professor, School of Pharmacy, Desh Bhagat University, Mandi Gobindgarh, Punjab

<sup>6</sup>Professor & Principal, School of Pharmacy, Desh Bhagat University, Mandi Gobindgarh, Punjab

<sup>7</sup>Associate Professor, School of Desh Bhagat University, Mandi Gobindgarh, Punjab

### Corresponding author-

<sup>\*</sup>Ajay Sehgal, Assistant Professor, School of Pharmaceutical Sciences, Om Sterling Global University, Hisar, Haryana, Email id: [ajaysehgal1803@gmail.com](mailto:ajaysehgal1803@gmail.com)

### Article History

Volume 6, Issue 4, 2024

Received: 12 June 2024

Accepted: 26 July 2024

doi:

[10.48047/AFJBS.6.4.2024.1237-1277](https://doi.org/10.48047/AFJBS.6.4.2024.1237-1277)

### ABSTRACT

The synthesis of novel derivatives of Yakuchinone B, a naturally occurring phenolic compound, presents a promising avenue in the search for effective anti-inflammatory agents. This research focuses on the design, synthesis, and evaluation of these derivatives to enhance their therapeutic potential against inflammation. Yakuchinone B, isolated from *Alpiniaoxyphylla* Miquel, has demonstrated notable anti-inflammatory properties, making it a valuable lead compound. However, its clinical application is limited by suboptimal pharmacokinetic properties and potential side effects. To overcome these limitations, a series of novel derivatives were synthesized through structural modifications aimed at improving their pharmacological profile. The synthetic approach involved modifying the phenolic and carbonyl functionalities of Yakuchinone B, exploring different substituents to optimize anti-inflammatory activity and reduce toxicity. The structural modifications were guided by computational modeling and structure-activity relationship (SAR) studies, which provided insights into the molecular interactions with key inflammatory mediators. The produced derivatives were analyzed utilizing spectroscopic techniques including NMR, FTIR, and MS to verify their

structures. The *in vitro* anti-inflammatory efficacy was assessed by measuring the suppression of pro-inflammatory cytokines, including TNF- $\alpha$ , IL-6, and IL-1 $\beta$ , in macrophages challenged with lipopolysaccharide (LPS). Additionally, the potential of these derivatives to inhibit key enzymes involved in the inflammatory response, including COX-2 and iNOS, was assessed. Selected

derivatives were further tested *in vivo* in animal models of inflammation to confirm their efficacy and safety. Preliminary results indicate that several novel derivatives of Yakuchinone B exhibit significantly enhanced anti-inflammatory activity compared to the parent compound. These findings suggest that structural modifications can successfully improve the pharmacological properties of Yakuchinone B, making these novel derivatives potential candidates for the development of new anti-inflammatory therapies. Further studies are warranted to optimize these derivatives and explore their mechanisms of action in greater detail.

**Keywords:** Yakuchinone B, Synthesis, Characterization, Antiinflammatory, Structure-activity relationship, *Insilico*

## INTRODUCTION

For a very long time, people have been worried about the dangers of inflammation. Inflammation is a normal biological process that happens no matter what causes it. It can be caused by painful tissues or a strong infection. In and of itself, it is a basic and important biochemical process of inflammation involves the production of white blood cells and essential chemicals that serve to defend the body against harmful germs and organisms. This bodily process is associated with various health issues such as Alzheimer's disease, heart disease, diabetic vascular complications (DVC), and other ailments. Inflammatory diseases, such as rheumatic fever, ankylosing spondylitis, osteoarthritis, systemic lupus erythematosus, rheumatoid arthritis, polyarthritis nodosa, and polyarthritis nodosa, can lead to symptoms like swelling, oedema, and infiltration of white blood cells. [2].

Depending on where it happens, inflammation can be inside or outside the body. IL-17 Inflammation is a crucial component of the body's immunological response. It is produced by many physiological mechanisms that are triggered by the immune system in response to illness or injury. One could say it's a way for the body to protect itself by getting rid of things that could be dangerous so that it can heal. It is the defensive reaction that the body uses to try to heal itself after getting hurt, protect itself against viruses and germs, and fix damaged tissue. People go through a lot of pain when this biological process gets worse, even though it is necessary for life. Redness, swelling, and warmth are some of the symptoms [3]. Pain and some stiffness are also present.

A chain of events involving the breakdown of arachidonic acid sets off inflammation During biological processes, proteins known as cytokines are synthesised as a means of urgent notification. They recruit the body's immune cells and nutrients and initiate responses in the body's surroundings to facilitate the resolution of the issue. Be aware that inflammation that lasts longer than it needs to may do more harm than good, so keep that in mind. People with autoimmune diseases, like arthritis, may have been in even more pain than thought, since these diseases attack the body's tissue. Anti-inflammatory drugs are rarely needed to ease pain and stop further reactions. [4].

Lipoxygenase and cyclooxygenase are two of the most significant enzymes involved in inflammatory responses. Prostaglandins, leukotrienes, and other mediators are synthesized by these enzymes, increasing inflammatory reactions, pain, and other symptoms. Both TXs and PCs are involved in the synthesis of prostanoid biosynthesis, whereas leukotriene production is enhanced by the latter. There are two kinds of inflammatory cytokines: COX-1 and COX-2. When the cyclooxygenase-1 (COX-1) enzyme is reduced, the pain, fever, and edema associated

with inflammatory disorders may be alleviated. Constantly expressed in the body, the COX-1 isoform of cyclooxygenase serves as a housekeeping isoform that regulates renal blood flow, protects the stomach from ulcers, and produces prostaglandin E<sub>2</sub> (PGE<sub>2</sub>) to preserve gastric mucosal surface coherence and structure [5].

Several external and intracellular physiological stimuli, including heat and cold, activate COX-2, an inducible early response gene. Additionally, IL-1, TNF, EGF, PAF, endothelin, and arachidonic acid have all been linked to the development of the disease. One of PGs' many jobs is to control inflammation, which they do in a number of different ways. NSAIDs, which stop COX-1 and COX-2 enzymes before they can work, are less efficient than COX-2 inhibitors in relieving inflammation and pain while also causing fewer unpleasant gastrointestinal effects. However, they have been related aspirin and other non-steroidal anti-inflammatory meds have been linked to a higher chance of stroke and heart attack. [6].

Dioxygenases and lipoxygenases that don't have hemethatis found in a wide range of animals, from plants and fungi to humans. The five lipoxygenases found in humans are the 5S-(arachidonate: oxygen 5-oxidoreductase), 12R-(arachidonate 12-lipoxygenase, 12R-type), 12S-(arachidonate: oxygen 12-oxidoreductase), and two distinct 15S-(arachidonate: oxygen 15-oxidoreductase). LOXs cause structural and metabolic changes in the cell that are linked to a wide spectrum of diseases. Non-heme iron dioxygenases, of which these enzymes are members, are involved in the production and, under certain conditions, how fatty acid hydroperoxides are broken down. It's interesting to look at the LOX family of enzymes because they help fatty acid substrates undergo stereospecific oxidation. A polyunsaturated fatty acid that has a cis-1,4-pentadiene structure is referred to as the LOX enzyme because it is responsible for the incorporation of oxygen. Many analogs may be identified by the number of carbons in each molecule that are replaced with oxygen, such as 5-LOX, 8-LOX, 12-LOX, and 15-LOX. The LOX enzymes, particularly the isoform 5-LOX, play a major role in inflammatory and allergic reactions, since it induces the production of the more potent inflammatory mediator, LTs. As a class of biologically active chemicals, these compounds are generated by basophils, neutrophils, leukocytes, mast cells (mast cells), and other tissues or cells in response to both immunological as well as non-immune stimuli. Many inflammatory and allergic diseases are helped by lymphocytes (LTs), which play an important role [7].

The 5-LOX-mediated leukotriene B<sub>4</sub> (LTB<sub>4</sub>) and peptidoleukotrienes produced in the body cause chemotaxis and severe bronchoconstriction. Many medical conditions, including psoriasis, rheumatoid arthritis, colitis ulcerosa, and allergic rhinitis, have been shown to have high levels of LTs. The most effective technique to reduce inflammation is to completely stop the manufacture of LT, which may be done either directly or indirectly by blocking the LOX pathway. Natural plant materials have been found in the ancient text, which has a host of assertions and prejudices and has been dated. Its etiology and treatment methods may be traced back to countless civilizations, demonstrating the constant and insurmountable challenges that mankind encounters on a daily basis. Before any preclinical research for anti-inflammatory activity was done on heterocycles other than aspirin, the miracle drug that made aspirin famous, other intriguing possibilities were available on the market [8].

In the realm of inflammatory illnesses, there exist several types of anti-inflammatory medications, including both steroidal and non-steroidal options. These substances have undergone extensive research to explore their medicinal potential, but their use remains limited because of issues with their pharmacokinetics, unwanted side effects, and other issues. People are always looking for a good anti-inflammatory drug using a number of acceptable means. This

illness is still a big worry, even though a lot of work has been put into finding new medicinal ways to treat different kinds of inflammation. So, it is very important to find new groups of anti-inflammatory drugs that work in specific ways. Controlling biological systems has been known for a long time to be an important way to learn about many different kinds of responses. Therefore, finding the processes and causes that stop inflammation is an interesting way to find possible anti-inflammatory drugs [9]. While the search for new drugs is never-ending, it has led to many hopeful ideas that have helped people a great deal. More than ten years ago, medicine growth in developing countries made a lot of progress. A lot of substances that were not known before have been looked into in depth, and there is still a great deal to learn about chemistry. The most hopeful method in modern drug creation is target-based production of new medicinal molecules. Herbal treatments have been used a lot to get patients to follow through with their plans, but the biological activity has been greatly reduced, and there have been no real benefits in terms of side effects. A lot of work has been put into rationally developing new non-steroidal anti-inflammatory options (NSAIC). In this case, the therapeutic potentials of many joined rings (four to five rings) need to be looked at and improved using rational methods [10].

More than a thousand NSAICs of various heterocycles have been recorded in chemical databases during the last decade. However, long-term usage of any of the molecules that have been examined and authorized in clinical trials has proven problematic due to a variety of issues. With regard to the long-term usage of modern medicines, there have been a few snags along the way. Patients who use anti-inflammatory medications for a long length of time face a variety of issues, including gastrointestinal discomfort, bleeding in the stomach, cardiac troubles, and more. COX-2 inhibitors may increase the risk of gastric and intestinal bleeding, ulceration, and perforation, which may be life-threatening. This may happen at any time over the course of treatment and there are no warning signs. Elderly patients have a greater chance of suffering this kind of reaction. Throughout time, other an increasing number of inhibitors have been created, but most of them have had similar side effects that make them less useful for long amounts of time because they show up in the same biochemical pathways. [11].

The aim of this work is to synthesize novel Yakuchinone B derivatives, characterize through sophisticated spectroscopic techniques, and screen for anti-inflammatory activity in Carrageenan-induced rat paw edema model.

## **2. MATERIALS AND METHODS**

### **2.1. Chemicals**

Yakuchinone B, Thionyl chloride, mesyl chloride, and tosyl chloride were procured from Sigma Aldrich Pvt. Ltd., Bangalore, India. Sodium hydroxide, carboxymethyl cellulose, carrageenan, dichloromethane, and saline (0.9%) were obtained from HiMedia Pvt. Ltd., located in Mumbai, India. Methanol, double distilled water, glacial acetic acid, and ethanol were obtained from HiMedia Pvt. Ltd., located in Mumbai, India.

### **2.2. Molecular Docking**

The molecular docking studies were performed as per the procedure put forward by Sharma et al., 2018 [12].

#### **2.2.1. Preparation of Ligand**

The models were made with the 2D-sketcher feature of the Schrodinger Software set 2021-2. The Maestro environment v.12.8 was used to look at docking. Standard drugs were downloaded from PubChem library and were uploaded in the Maestro environment. LigPrep software was

used to generate stereoisomers of these ligands. A maximum of 4 poses was generated for each ligand to the right protonation states at a pH level of 7.0 using the Epikioniser. The OPLS 2005 force field was used to make tautomerised, desalted ligands that kept the necessary chiralities of the input files. This led to the creation of an optimised low-energy 3D ligand. Using bendable ligands and mobile protein atoms, the method solved the docking problem.

### **2.2.2. Preparation of Protein**

The Protein Data Bank (PDB) was used to download several 3D solid target shapes. The target was made by taking out all the water molecules that were bigger than  $5\text{\AA}$ , giving disulphideThe structure may be analysed by examining the linkages, bond order, and formal charges, while excluding the metal ions, co-factors, and heterogroups. The hydrogen atoms and the hydrogen-bonding network were enhanced by the use of the H-bond assignment technique. Molecular docking was used to determine the receptor patterns for protein targets and identify the specific locations where the ligand would interact with the anticipated active site. The grids, which are square boxes with defined dimensions, include the whole ligand and were positioned at the core of the ligand (where it formed crystals with the desired structure). In order to include all the amino acid residues present in rigid structures, the dimensions of the grid box were increased to  $126\text{\AA}$  (x),  $126\text{\AA}$  (y), and  $126\text{\AA}$  (z). The angular separation between each grid point was  $0.375^\circ$ . The minimum charge was established at 0.25, while the Van der Waals scale factor was set at 1. Induced-fit docking (IFD) was performed for each ligand, and the best-docked posture with the lowest score was subsequently confirmed.

### **2.2.3. Induced-Fit Molecular Docking (IFD)**

The IFD was made using a method called structure-based drug design. This method includes making exact shape molecules that can attach to the known the shape of an organic target. To do this, we put the free-state molecules into the active site, enzyme, tube, etc., to get a picture of how they would bind and check how well they fit. We use receptor-based computer methods to figure out how to link something that binds a large protein to a small one. This is important because it helps us find the best relationship with the fewest possible physical problems. A maximum of 10 conformers were looked at during the docking process. The community was limited to 150 people, who were chosen at random. Change rate was set to 0.02, and crossing rate was set to 0.8. It was set so that there could be a maximum of 500000 energy ratings, 1000 generations, and 1 top person who naturally survived. Moves were broken up into  $0.2^\circ$  steps, quaternions into  $5^\circ$  steps, and torsions into  $5^\circ$  steps. It was set to 10,000 tries, the external grid energy was set to 1000.0, and 10 LGA runs were made. It was looked into how the docked structure interacts and how much energy it needs to join. It was done several times to get different stopped shapes and to figure out how much docking energy was expected. From the docked structures, the best ligand-receptor structure was picked based on the ligand's low energy and how easily it could interact with solvents. Based on the information received, the chemicals were rated, and some of them were tested in the lab to see if they had biological action. The Glide Score was found for each ligand.

## **2.3. Computational studies**

The computational studies were performed as per the procedure put forward by Deokar and Shaikh, 2022 [13].

### **2.3.1. Pharmacokinetics, Bioavailability, and Drug-likeness studies**

The SwissADME online tool was used to make predictions about pharmacokinetics, specifically ADME, absorption, and how much ligands are like drugs. The technology uses six physical

properties—lipophilicity, size, polarity, insolubility, flexibility, and insaturation—to figure out how similar a substance is to a drug. Some ADME features were found to be positive or negative in the BOILED-Egg model. These included inactive human gut absorption (HIA) and blood-brain barrier (BBB) diffusion, as well as substrate or non-substrate of the permeability glycoprotein (P-gp). Various methods may be used to determine the lipophilicity of a substance, such as the calculation of Log p/w utilising parameters like iLOGP and the generalized-born and solvent accessible surface area (GB/SA) model. XLOGP3 is a molecular modelling technique that incorporates correction variables and uses a library based on knowledge. WLOGP is a completely atomistic method implementation. MLOGP is an example of a topological approach that relies on. The Lipinski (Pfizer) filter, the first rule-of-five incorporated into a tool, was used to estimate the drug-like properties of a substance. Many physical and chemical factors were used to figure out what the bioavailability radar would say about the bioavailability of a drug when taken by mouth. There were ranges for each parameter: LIPO (lipophilicity) ranged from -0.7 to +5.0; SIZE (size) ranged from 150gm/mol to 500gm/mol; POLAR (polarity) ranged from 20Å<sup>2</sup> to 130Å<sup>2</sup>; INSOLU (not soluble in water) ranged from 0 to 6 on the log S scale; INSATU (not saturated or insaturation) ranged from 0.3 to 1 on the fraction of carbons in the sp<sup>3</sup> hybridisation fraction; and FLEX (flexibility) ranged from 9. Number of links that can be rotated = 0.

### **2.3.2. Drug Target Identifications**

SwissTargetPrediction is a web service that predicts the targets of bioactive small molecules. This website lets you guess where a tiny molecule will go. It uses a mix of 2D and 3D similarity measures to match the question molecule to a collection of 280,000 molecules that are active on more than 2000 targets across five different species. To figure out the chemical processes that cause bioactivity and to predict possible side effects or cross-reactivity, it is necessary to map out the targets of bioactive small molecules. Three different animals (models) have been used to make predictions. For close paralogs and orthologs, it is possible to map forecasts by homology within and between species. People (*Homo sapiens*), rats (*Rattus norvegicus*), and mice (*Mus musculus*) have all been shown to have good ligand targets that stop them from working.

### **2.4. Molecular simulation study of the most promising compound using Gromacs® software**

The GROMACS modelling package and the CHARMM 27 force field were used to simulate the ligand's molecular motion. To get a molecular topology file that works with the CHARMM 27 force field, the SwissParam web service was used to specify the water model. The protein-ligand assembly was then solvated, and the whole system was neutralised by adding Na ions to replace the water molecules. Following these steps, the system's energy minimisation was carried out. Next, the system was balanced by running two NVT (5 ns) and NPT (5 ns) runs in a row. It was set to 298 K with the V-rescale thermostat and 1 bar of pressure with the Berendsenbarostat for all NVT and NPT runs. Finally, the groups that were made were put through a 40ns MD simulation with a 2-fs time step for each trial. An 1 nm cut-off ratio and the smooth Particle Mesh Ewald (PME) procedure were used to deal with the long-range electric interactions. Visual molecular dynamics (VMD) software was used to look at pictures of simulated paths. XMGRACE was used to plot the root mean square deviation (RMSD), radius of gyration (Rg), and root mean square variation (RMSF) values of peptide (atom backbone). [14].

### **2.5. Synthesis of molecules**

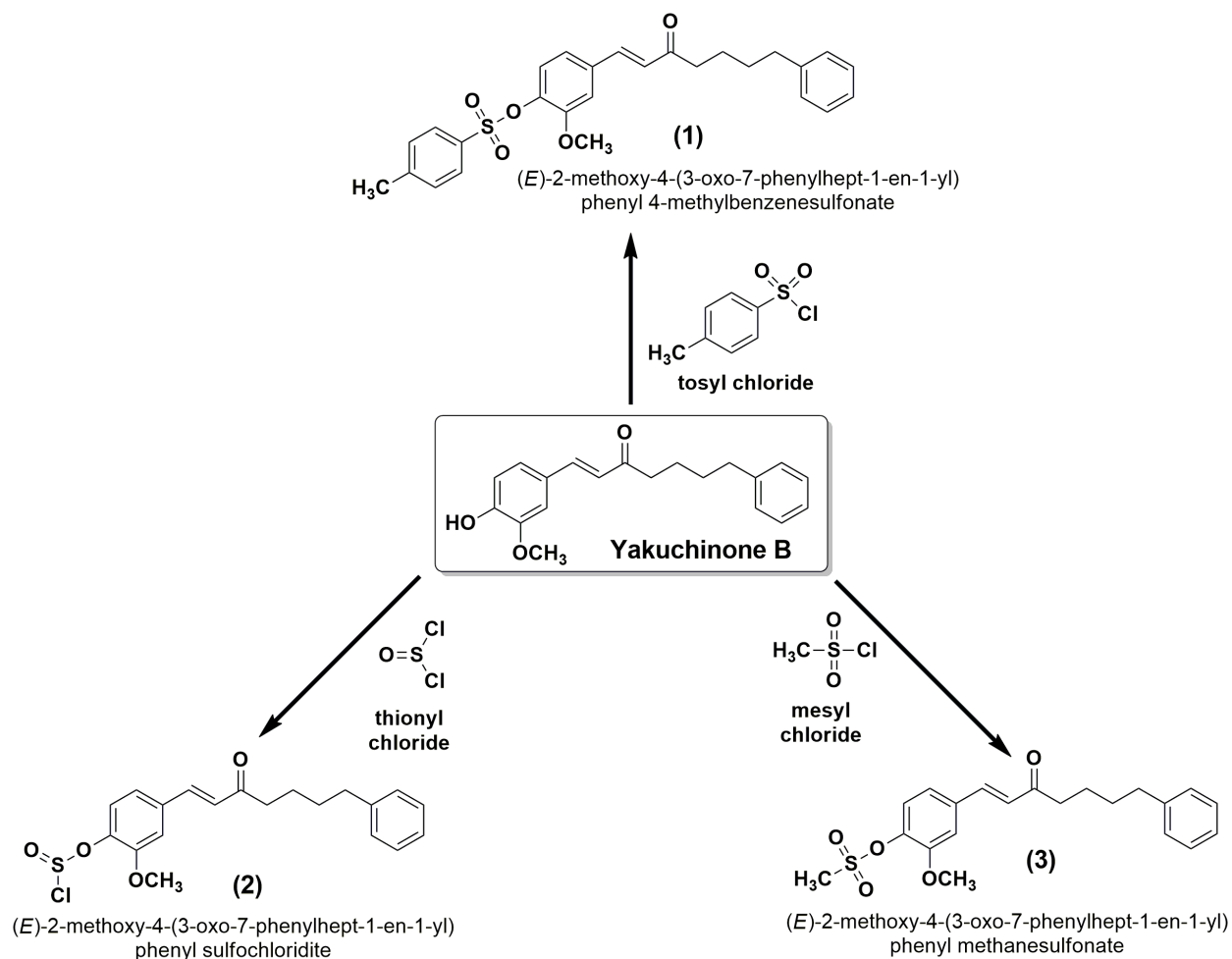


**Figure 1.** Synthesis of novel Yakuchinone B derivatives.

### 2.5.1. Synthesis of *(E)*-2-methoxy-4-(3-oxo-7-phenylhept-1-en-1-yl)phenyl 4-methylbenzenesulfonate

To a stirred solution of the Yakuchinone B (1 mmol) and tosyl chloride (1.2 mmol) in  $\text{CH}_2\text{Cl}_2$  (5 mL), at  $0^\circ\text{C}$ ,  $\text{Et}_3\text{N}$  (5 mmol) was added dropwise. After 1 hr the reaction mixture was diluted with  $\text{H}_2\text{O}$  (10 mL) and extracted with  $\text{CH}_2\text{Cl}_2$  ( $3 \times 5$  mL). The combined organic layers were washed with  $\text{H}_2\text{O}$  ( $2 \times 5$  mL), brine ( $2 \times 5$  mL), dried ( $\text{Na}_2\text{SO}_4$ ) and evaporated.

FTIR: 3274 (-NH, stretch), 3128 (C-H, aromatic), 1737 (C=O), 1701 (C-N, stretch), 1688 (C=C, aromatic), 1620 (C=C, aromatic), 1562 (-NH, bending), 1488 (-CH<sub>2</sub>), 1208 (C-O); <sup>1</sup>H-NMR:  $\delta$  0.99 (3H, t,  $J = 7.4$  Hz), 2.65 (2H, q,  $J = 7.4$  Hz), 7.10-7.32 (5H, 7.16 (dddd,  $J = 7.8, 1.3, 1.0, 0.5$  Hz), 7.20 (tt,  $J = 7.7, 1.3$  Hz), 7.26 (tdd,  $J = 7.7, 1.6, 0.5$  Hz)); <sup>13</sup>C-NMR:  $\delta$  11.3 (1C, s), 15.8 (1C, s), 20.3-20.4 (2C, 20.4 (s), 20.4 (s)), 21.3 (1C, s), 26.3-26.4 (2C, 26.4 (s), 26.4 (s)), 29.1 (1C, s), 35.6 (1C, s), 40.6 (1C, s), 41.8 (2C, s), 59.6 (1C, s), 117.9 (2C, s), 119.3 (1C, s), 119.9 (1C, s), 127.1 (1C, s), 129.0 (1C, s), 129.6 (2C, s), 139.4 (1C, s), 141.5 (1C, s), 142.0 (1C, s), 144.9 (1C, s); Mass:  $m/z$  329; Fragments: 389.19, 373.19, 321.09, 300.19, 287.19; CHN Analysis: Theoretical: C, 64.39; H, 5.20; Cl, 7.31; O, 16.49; S, 6.61; Practical: C, 61.14; H, 4.99.

### 2.5.2. Synthesis of *(E)*-2-methoxy-4-(3-oxo-7-phenylhept-1-en-1-yl)phenylsulfochloridite

To a stirred solution of the Yakuchinone B (1 mmol) and thionyl chloride (1.2 mmol) in  $\text{CH}_2\text{Cl}_2$  (5 mL), at  $0^\circ\text{C}$ ,  $\text{Et}_3\text{N}$  (5 mmol) was added dropwise. After 1 hr the reaction mixture was diluted with  $\text{H}_2\text{O}$  (10 mL) and extracted with  $\text{CH}_2\text{Cl}_2$  ( $3 \times 5$  mL). The combined organic layers were washed with  $\text{H}_2\text{O}$  ( $2 \times 5$  mL), brine ( $2 \times 5$  mL), dried ( $\text{Na}_2\text{SO}_4$ ) and evaporated.

FTIR: 3280 (-NH, stretch), 3168 (C-H, aromatic), 1791 (C=O), 1713 (C-N, stretch), 1681 (C=C, aromatic), 1644 (C=C, aromatic), 1599 (-NH, bending), 1489 (- $\text{CH}_2$ ), 1272 (C-O);  $^1\text{H-NMR}$ :  $\delta$  0.93-1.05 (6H, 0.99 (d,  $J = 6.7$  Hz), 0.99 (d,  $J = 6.7$  Hz)), 1.18-1.32 (2H, 1.25 (dd,  $J = 7.7, 7.2$  Hz), 1.25 (dd,  $J = 7.7, 7.2$  Hz)), 1.52 (1H, tsept,  $J = 7.2, 6.6$  Hz), 1.70 (1H, dtt,  $J = 14.1, 8.9, 6.7$  Hz), 1.85-2.31 (11H, 1.93 (dtt,  $J = 14.1, 6.7, 2.3$  Hz), 2.08 (ddd,  $J = 14.6, 6.7, 2.3$  Hz), 2.08 (ddd,  $J = 14.5, 6.7, 2.3$  Hz), 2.23 (ddd,  $J = 14.6, 8.9, 6.7$  Hz), 2.23 (ddd,  $J = 14.5, 8.9, 6.7$  Hz), 2.25 (s)), 2.80 (1H, t,  $J = 7.7$  Hz), 3.75 (3H, s), 6.29 (2H, ddd,  $J = 8.2, 1.1, 0.5$  Hz), 6.67 (2H, ddd,  $J = 8.7, 2.7, 0.5$  Hz), 7.04-7.17 (4H, 7.10 (ddd,  $J = 8.7, 1.7, 0.5$  Hz), 7.11 (ddd,  $J = 8.2, 1.1, 0.5$  Hz));  $^{13}\text{C-NMR}$ :  $\delta$  15.8 (1C, s), 22.5-22.6 (2C, 22.6 (s), 22.6 (s)), 24.4 (1C, s), 26.3-26.4 (2C, 26.4 (s), 26.4 (s)), 35.1 (1C, s), 40.6 (1C, s), 41.8 (2C, s), 56.0 (1C, s), 60.1 (1C, s), 114.5 (2C, s), 117.9 (2C, s), 120.5 (2C, s), 127.4 (2C, s), 141.9-142.1 (2C, 142.0 (s), 142.0 (s)), 144.9 (1C, s), 159.8 (1C, s); Mass:  $m/z$  350; Fragments: 256.19, 186.19, 127.09, 101.29; CHN Analysis: Theoretical: C, 61.14; H, 5.39; Cl, 9.02; O, 16.29; S, 8.16; Practical: C, 59.12; H, 5.03.

### 2.5.3. Synthesis of (*E*)-2-methoxy-4-(3-oxo-7-phenylhept-1-en-1-yl)phenylmethanesulfonate

To a stirred solution of the Yakuchinone B (1 mmol) and mesyl chloride (1.2 mmol) in  $\text{CH}_2\text{Cl}_2$  (5 mL), at  $0^\circ\text{C}$ ,  $\text{Et}_3\text{N}$  (5 mmol) was added dropwise. After 1 hr the reaction mixture was diluted with  $\text{H}_2\text{O}$  (10 mL) and extracted with  $\text{CH}_2\text{Cl}_2$  ( $3 \times 5$  mL). The combined organic layers were washed with  $\text{H}_2\text{O}$  ( $2 \times 5$  mL), brine ( $2 \times 5$  mL), dried ( $\text{Na}_2\text{SO}_4$ ) and evaporated.

FTIR: 3299 (-NH, stretch), 3183 (C-H, aromatic), 1754 (C=O), 1734 (C-N, stretch), 1698 (C=C, aromatic), 1667 (C=C, aromatic), 1576 (-NH, bending), 1495 (- $\text{CH}_2$ ), 1213 (C-O);  $^1\text{H-NMR}$ :  $\delta$  0.93-1.05 (6H, 0.99 (d,  $J = 6.7$  Hz), 0.99 (d,  $J = 6.7$  Hz)), 1.18-1.32 (2H, 1.25 (dd,  $J = 7.7, 7.2$  Hz), 1.25 (dd,  $J = 7.7, 7.2$  Hz)), 1.52 (1H, tsept,  $J = 7.2, 6.6$  Hz), 1.70 (1H, dtt,  $J = 14.1, 8.9, 6.7$  Hz), 1.85-2.31 (14H, 1.93 (dtt,  $J = 14.1, 6.7, 2.3$  Hz), 2.08 (ddd,  $J = 14.6, 6.7, 2.3$  Hz), 2.08 (ddd,  $J = 14.5, 6.7, 2.3$  Hz), 2.23 (ddd,  $J = 14.6, 8.9, 6.7$  Hz), 2.23 (ddd,  $J = 14.5, 8.9, 6.7$  Hz), 2.21 (s), 2.25 (s)), 2.80 (1H, t,  $J = 7.7$  Hz), 6.21-6.35 (4H, 6.27 (ddd,  $J = 8.2, 1.4, 0.5$  Hz), 6.29 (ddd,  $J = 8.2, 1.1, 0.5$  Hz)), 7.06 (2H, ddd,  $J = 8.2, 1.3, 0.5$  Hz), 7.21 (2H, ddd,  $J = 8.2, 1.1, 0.5$  Hz);  $^{13}\text{C-NMR}$ :  $\delta$  15.8 (1C, s), 21.3 (1C, s), 22.5-22.6 (2C, 22.6 (s), 22.6 (s)), 24.4 (1C, s), 26.3-26.4 (2C, 26.4 (s), 26.4 (s)), 35.1 (1C, s), 40.6 (1C, s), 41.8 (2C, s), 60.1 (1C, s), 117.9-118.0 (4C, 117.9 (s), 117.9 (s)), 127.4 (2C, s), 129.6 (2C, s), 141.5 (1C, s), 141.9-142.1 (2C, 142.0 (s), 142.0 (s)), 144.9 (1C, s); Mass:  $m/z$  366; Fragments: 219.09, 173.19, 149.19, 141.19; CHN Analysis: Theoretical: C, 64.93; H, 6.23; O, 20.59; S, 8.25; Practical: C, 60.54; H, 5.93.

## 2.6. Characterization of compounds

The synthesized molecules was characterized in terms of Yield (from the formula; Practically obtained weight / Theoretically calculated weight  $\times 100$ ), Appearance (colour and state), Melting point (calculated using Thiele's tube method), and Retention factor (based on optimized chromatographic solvent system). The synthesized molecules was comprehensively characterized using sophisticated analytical techniques such as Fourier-transformed Infrared (FT-IR) Spectroscopy, Proton-Nuclear Magnetic Resonance ( $^1\text{H-NMR}$ ) Spectroscopy, Carbon-Nuclear Magnetic Resonance ( $^{13}\text{C-NMR}$ ) Spectroscopy, and Mass Spectroscopy; where specific peaks was studied to establish the chemical structures of the newly synthesized molecules. CHN-



Elemental Analysis was used to determine Carbon, Hydrogen, and Nitrogen compositions (in %) in the molecules and compare with the theoretically calculated values.

## 2.7. Anti-inflammatory activity

### 2.7.1. Animals

The anti-inflammatory activity of the novel compounds was screened after obtaining ethical permission from the institution. As per the screening protocol, albino rats of the same sex of weight 180-250 g were employed. The animals were kept in polypropylene cages under hygienic condition at controlled temperature and humidity of 25–26°C / 50–55%. A 12/12 hrs light/dark cycle was also maintained. The animal ethical permission was obtained from Departmental / Institutional Animal Ethical in compliance with Committee for the Purpose of Control and Supervision of Experiments on Animals (CPCSEA).

### 2.7.2. Anti-inflammatory screening

As per the procedure, the normal carrageenan-induced paw oedema method was used to test the molecules' ability to reduce inflammation in living organisms. In order to make the oedema less unpredictable, the rats were not fed for the whole night. Five millilitres of purified water were given to each person by mouth before the testing began. At first, 100 mg/kg of body weight of the test substance was mixed with water solution and given by mouth an hour before inflammation was caused. By introducing a 1% carrageenan solution under the skin, the inflammation was caused in the subplanter area of the rats' right hind paw. As part of the study, the thickness of each rat paw was tested three times, once every hour, for three hours in order to find the oedema. The difference in thickness between paws that were injected and paws that were not injected shows how well the chemicals might work at lowering the swelling. The collected values were shown as mean + standard error. The saltwater solution with a few drops of Tween 80 will be given to the comparison group. [15].

The percent edema inhibition was calculated using following equation.

$$\% \text{ Edema inhibition} = (1 - V_t/V_c) \times 100$$

Where,  $V_t$  = Mean edema volume of test group,  $V_c$  = Mean edema volume of test group.

## 2.8. Statistical analysis of the results

All the data was represented in Mean  $\pm$  SD. Data was analyzed using one-way ANOVA followed by Dunnett's multiple comparison tests using Sigmasat® software. The group means was considered significantly significant when p-value is  $< 0.05$

## 3. RESULTS AND DISCUSSION

### 3.1. Pharmacokinetics, Bioavailability, and Drug-likeness studies

#### 3.1.1. Compound-1

**Table 1** Describes the predictive values for pharmacokinetics, solubility, and drug-likeness data on a new compound derived from Yakuchinone B. Molecule 1 had a high rate of absorption. The LogP value showed that there was good blood-brain permeability, and a low negative value meant that there was less skin absorption. The molecule did not show that it was a p-glycoprotein substrate when it came to metabolism. It stops CYP450 from working and especially stops CYP1A2 and CYP2D6 isoforms. It was possible to identify absorption and drug-likeness with a modest bioavailability number. It was found that the new Yakuchinone B version wasn't very water-soluble.

### 3.1.2. Compound-2

Molecule 2 had a high rate of uptake. The LogP value showed that there was good blood-brain permeability, while a moderately negative value showed that there was less skin absorption. It turned out that the molecule was a p-glycoprotein substrate in the case of metabolism. It stops CYP450 from working and especially stops CYP2D6 gene. To guess absorption and drug-likeness, a modest bioavailability number of 0.55 was found. This new Yakuchinone B compound was found to have poor to middling water solubility properties.

### 3.1.3. Compound-3

The molecule-3 (**Figure 2**) showed low rate of absorption. The LogP value showed that there was poor blood-brain permeability, and a low negative value meant that there was less skin absorption. It turned out that the molecule was a p-glycoprotein substrate in the case of metabolism. It stops CYP450 from working and especially stops CYP2C19 and CYP2D6 isoforms. To guess absorption and drug-likeness, a modest bioavailability number of 0.55 was found. It was found that the new Yakuchinone B version wasn't very water-soluble.

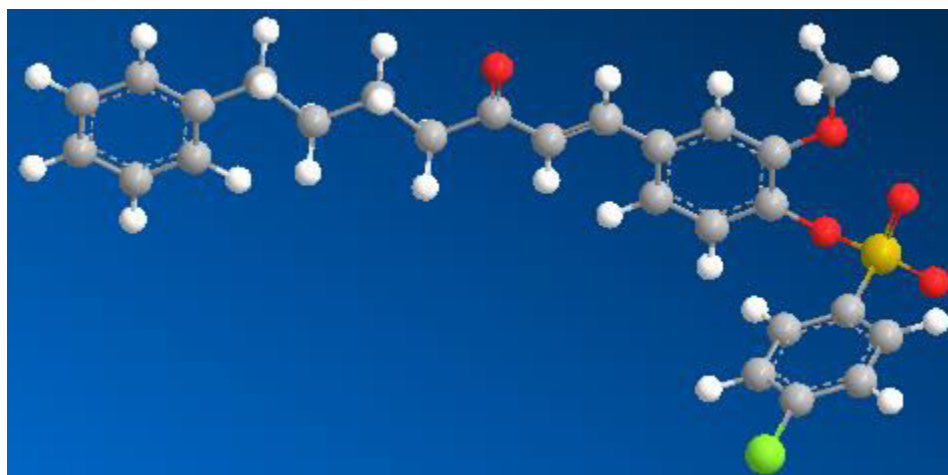
**Table 1.** Pharmacokinetics and physicochemical properties of novel Yakuchinone B derivatives.

| PROPERTIES                        | Compound-1  | Compound-2   | Compound-3  |
|-----------------------------------|---|--|---|
| <b>Physicochemical Properties</b> |   |  |   |
| Formula                           | C <sub>26</sub> H <sub>25</sub> ClO <sub>5</sub> S                                | C <sub>20</sub> H <sub>21</sub> ClO <sub>4</sub> S               | C <sub>21</sub> H <sub>24</sub> O <sub>5</sub> S                |
| Molecular weight (g/mol)          | 484.11  | 392.08   | 388.13  |
| Number of heavy atoms             | 26  | 27   | 26  |
| Number of aromatic heavy atoms    | 12  | 12   | 12  |
| Fraction Csp <sup>3</sup>         | 0.48  | 0.50   | 0.50  |
| Number of rotatable bonds         | 7   | 8  | 7   |
| Number of H-bond acceptors        | 2   | 2  | 1   |
| Number of H-bond donors           | 2   | 1  | 1   |
| Molar Refractivity                | 111.71  | 116.18   | 114.65  |
| TPSA (Å <sup>2</sup> )            | 35.05   | 24.50  | 15.27   |
| SMILES                            | <chem>O=C(CCCCC1=CC=C(C=C1)/C=C/C2=CC=C(OS(C3=CC=C(Cl)C=C3)(=O)=O)C(OC)=C2</chem> | <chem>O=C(CCCCC1=CC=C(C=C1)/C=C/C2=CC=C(OS(Cl)=O)C(OC)=C2</chem> | <chem>O=C(CCCCC1=CC=CC=C1)/C=C/C2=CC=C(OS(=O)=O)C(OC)=C2</chem> |
| <b>Lipophilicity</b>              |   |  |   |
| Log Po/w (Ilog p)                 | 3.67  | 4.42   | 4.40  |
| Log Po/w (XLOGP3)                 | 5.99  | 6.32   | 6.71  |
| Log Po/w (WL)                     | 5.53  | 5.84   | 6.14  |

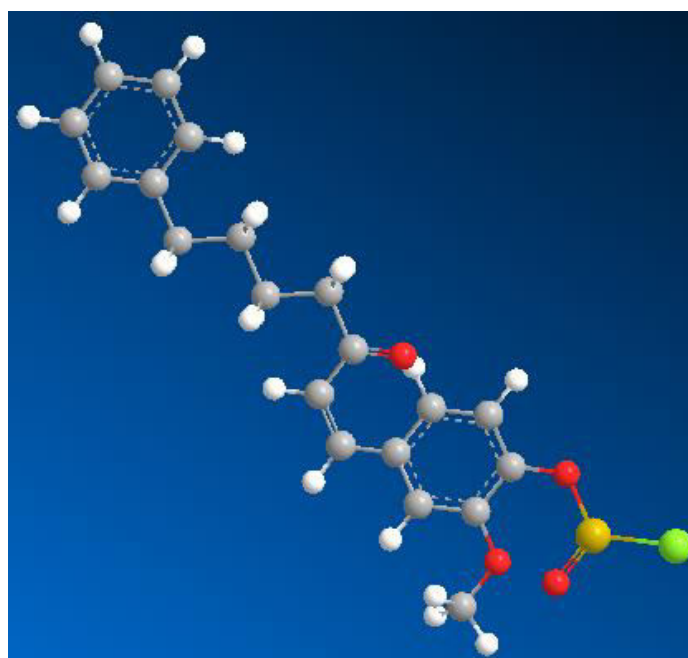
|                                 |                                |                                 |                                 |
|---------------------------------|--------------------------------|---------------------------------|---------------------------------|
| OGP)                            |                                |                                 |                                 |
| Log Po/w (ML OGP)               | 4.05                           | 4.26                            | 4.87                            |
| Log Po/w (SIL ICOS-IT)          | 4.65                           | 5.20                            | 5.66                            |
| Consensus Log Po/w              | 4.78                           | 5.21                            | 5.56                            |
| <b>Water Solubility</b>         |                                |                                 |                                 |
| Log S (ESOL)                    | -5.68                          | -5.90                           | -6.12                           |
| Solubility                      | 7.39e-04 mg/ml ; 2.09e-06mol/l | 4.67e-04 mg/ml ; 1.27e-06 mol/l | 2.66e-04 mg/ml ; 7.58e-07 mol/l |
| Class                           | Moderate Soluble               | Moderate Soluble                | Poorly Soluble                  |
| Log S (Ali)                     | -6.51                          | -6.62                           | -6.83                           |
| Solubility                      | 1.08e-04 mg/ml ; 3.07e-07mol/l | 8.71e-05 mg/ml ; 2.38e-07 mol/l | 5.13e-05 mg/ml ; 1.46e-07 mol/l |
| Class                           | Poorly Soluble                 | Poorly Soluble                  | Poorly Soluble                  |
| Log S (SILICO S-IT)             | -6.83                          | -7.53                           | -7.80                           |
| Solubility                      | 5.17e-05 mg/ml ; 1.47e-07mol/l | 1.09e-05 mg/ml ; 2.97e-08 mol/l | 5.58e-06 mg/ml ; 1.59e-08 mol/l |
| Class                           | Poorly Soluble                 | Poorly Soluble                  | Poorly Soluble                  |
| <b>Pharmacokinetics</b>         |                                |                                 |                                 |
| GI absorption                   | High (93.747%)                 | High (94.736%)                  | Low (83.636%)                   |
| BBB permeant                    | Yes (-0.942)                   | Yes (-0.168)                    | No                              |
| CNS permeability                | -2.159                         | -2.337                          | -2.281                          |
| P-gp substrate                  | No                             | Yes                             | Yes                             |
| Caco2 permeability              | 0.421                          | 1.131                           | 0.943                           |
| CYP1A2 inhibitor                | Yes                            | No                              | No                              |
| CYP2C19 inhibitor               | No                             | No                              | Yes                             |
| CYP2C9 inhibitor                | No                             | No                              | No                              |
| CYP2D6 inhibitor                | Yes                            | Yes                             | Yes                             |
| CYP3A4 inhibitor                | No                             | No                              | No                              |
| Log Kp (skin permeation) (cm/s) | -4.20                          | -4.05                           | -3.67                           |
| Total clearance (log            | -0.317                         | -0.106                          | -0.462                          |

|  |                           |                                     |                                      |
|--|---------------------------|-------------------------------------|--------------------------------------|
| ml/min/kg)   |                           |                                     |                                      |
| Renal OCT2 substrate                                 | No                        | No                                  | No                                   |
| <b>Toxicity</b>                                      |                           |                                     |                                      |
| Minnow toxicity (log mM)                             | -1.583                    | -1.013                              | -1.083                               |
| <i>T. pyriformis</i> toxicity (log ug/L)             | 0.295                     | 1.099                               | 1.259                                |
| Oral Rat Acute Toxicity (LD <sub>50</sub> ) (mol/kg) | 2.349                     | 2.577                               | 2.667                                |
| Oral Rat Chronic Toxicity (LOAEL) (log mg/kg_bw/day) | 1.17                      | 1.287                               | 1.374                                |
| Max. tolerated dose (human) (log mg/kg/day)          | 0.321                     | 0.787                               | 0.344                                |
| Hepatotoxicity                                       | No                        | No                                  | No                                   |
| Skin Sensitisation                                   | No                        | No                                  | No                                   |
| AMES toxicity  | No                        | No                                  | No                                   |
| <b>Drug-likeness</b>                                 |                           |                                     |                                      |
| Lipinski   | Yes; 0 violation          | Yes; 1 violation: MLOGP>4.15        | Yes; 1 violation: MLOGP>4.15         |
| Ghose  | Yes                       | No; 1 violation: WLOGP>5.6          | No; 1 violation: WLOGP>5.6           |
| Veber  | Yes                       | Yes                                 | Yes                                  |
| Egan   | Yes                       | Yes                                 | No; 1 violation: WLOGP>5.88          |
| Muegge   | No; 1 violation: XLOGP3>5 | No; 1 violation: XLOGP3>5           | No; 1 violation: XLOGP3>5            |
| Bioavailability Score                                | 0.55                      | 0.55                                | 0.55                                 |
| <b>Medicinal Chemistry</b>                           |                           |                                     |                                      |
| PAINS  | 0 alert                   | 0 alert                             | 0 alert                              |
| Brenk  | 1 alert: hydroquinone     | 0 alert                             | 0 alert                              |
| Lead-likeness  | No; 2 violations: MW>350, | No; 3 violations: MW>350, Rotors>7, | No; 2 violations: MW>350, XLOGP3>3.5 |

|                         | XLOGP3>3.5 | XLOGP3>3.5 |      |
|-------------------------|------------|------------|------|
| Synthetic accessibility | 3.19       | 3.30       | 3.28 |



**(Compound-1)**



**(Compound-2)**



(Compound-3)

Figure 2.3D representation of novel Yakuchinone B derivatives.

### 3.2. Bioavailability Radar Plot

#### 3.2.1. Compound-1

It was predicted that the drug would not be bioavailable when taken by mouth based on its INSATU value of 0.48, its FLEX value of 7, its INSOLU Logs (ESOL) value of -5.68 (not soluble), its SIZE value of 329.04 (molecular weight), its POLAR value of 35.05 (TPSA), and its LIPO value of 5.99 (XLOGP3 value). (Figure 3A).

#### 3.2.2. Compound-2

It was found that the bioavailability radar for oral bioavailability prediction had the desired INSATU value of 0.50, FLEX value of 8 rotatable bonds, INSOLU Logs (ESOL) value of -5.90 (insoluble), SIZE value of 366.54 g/mol, POLAR value of 24.50 Å<sup>2</sup>, and LIPO value of 6.32. (Figure 3B).

#### 3.2.3. Compound-3

To figure out how bioavailable a substance is when taken by mouth, the bioavailability radar showed that the desired INSATU value was 0.50, the number of rotatable bonds was 7, the insoluble logs (ESOL) value was -6.12, the molecular weight (g/mol) value was 350.54, the polar value was 15.27, and the lipoprotein (LIPO) value was 6.71. (Figure 3C).

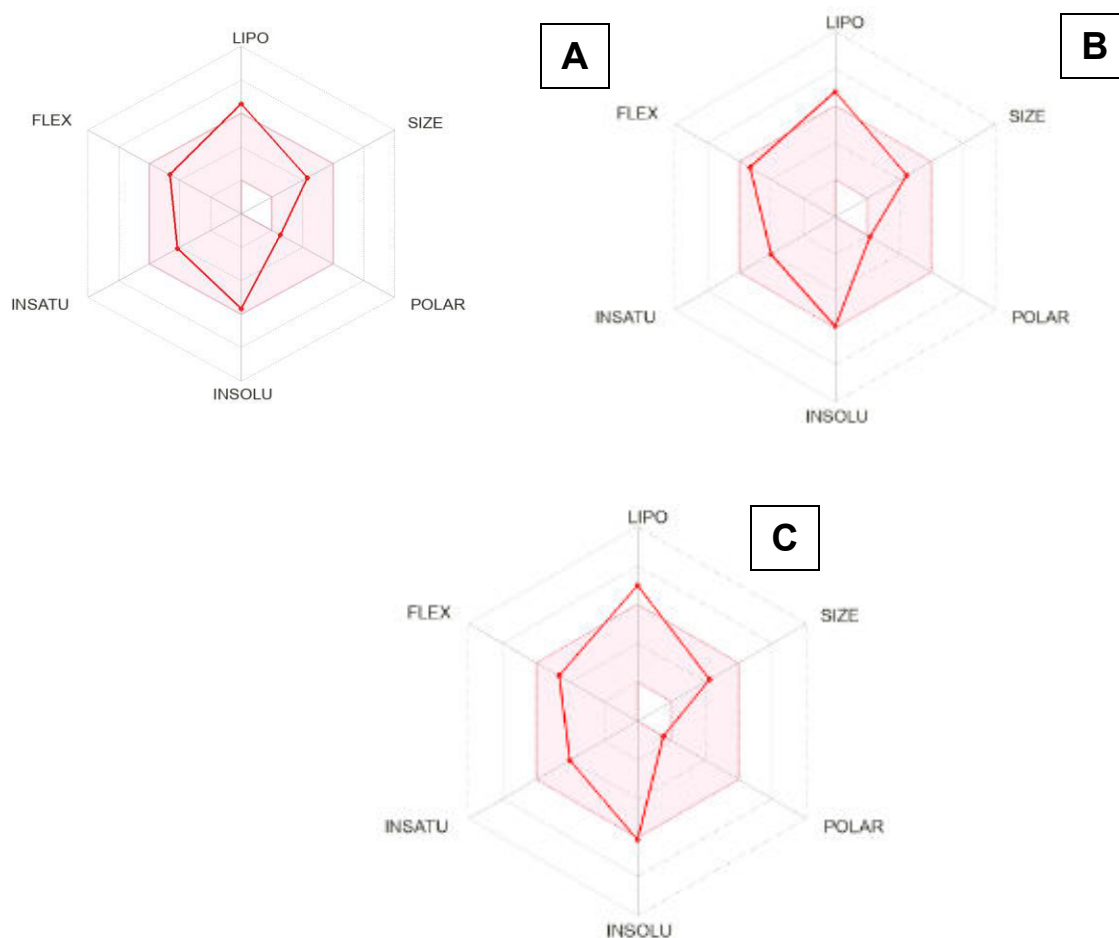


**Figure 3.** Bioavailability Radar Plot (A) Compound-1, (B) Compound-2, and (C) Compound-3.

### 3.3. Boiled Egg Plot

In case of BOILED-Egg model (Figure 4), Brain OrIntestinaLEstimated permeation method (BOILED-Egg) has already been suggested as a good way to make predictions. It does this by using computers to guess how lipophilic and polar small molecules are. Based on the absorption radar and BOILED-Egg image, the new Yakuchinone B product may be a good option for a drug.

#### 3.3.1. Compound-1

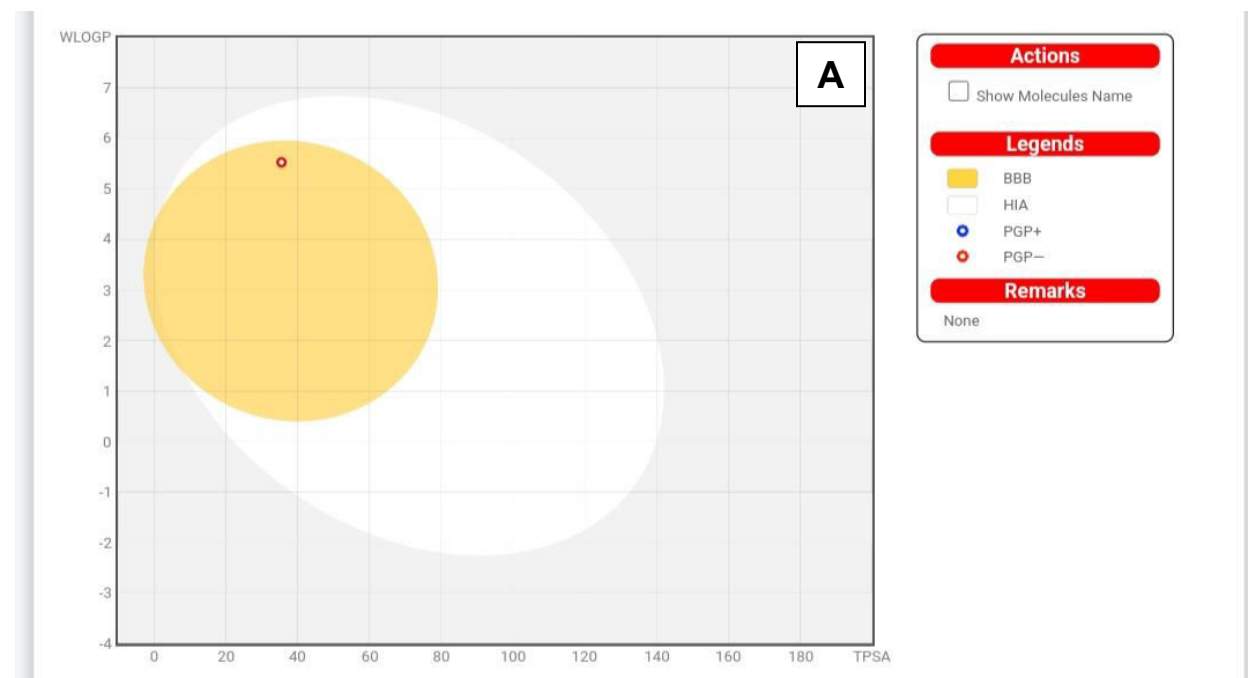
It was observed in the predictions that compound-1 (Figure 4A) was a PGP positive non-substrate. PGP positive non-substrate molecules are compounds that interact with P-glycoprotein but are not themselves transported by it. These molecules can influence PGP activity in several ways, such as inhibiting or activating its transport function, altering its expression levels, or modulating its conformation. Unlike substrates that are actively pumped out of cells by PGP, non-substrate molecules bind to PGP and affect its function without being expelled.

#### 3.3.2. Compound-2

It was obtained that novel Yakuchinone B derivative, compound-2 (Figure 4B) has limited ability to cross the blood-brain barrier and didn't absorb well in the digestive tract either. It was found that the molecule was PGP positive as a non-substrate in the model.

### 3.3.3. Compound-3

PGP positive non-substrate behaviour was observed in the predictions for compound-3 (**Figure 4C**). PGP positive non-substrate molecules represent a significant area of interest in pharmacology and drug development. By modulating the function and expression of P-glycoprotein, these molecules offer potential strategies for overcoming multidrug resistance, optimizing drug pharmacokinetics, and enhancing therapeutic efficacy. Ongoing research continues to explore and develop new PGP inhibitors and modulators, aiming to address the challenges posed by drug resistance and improve patient outcomes across various medical conditions.





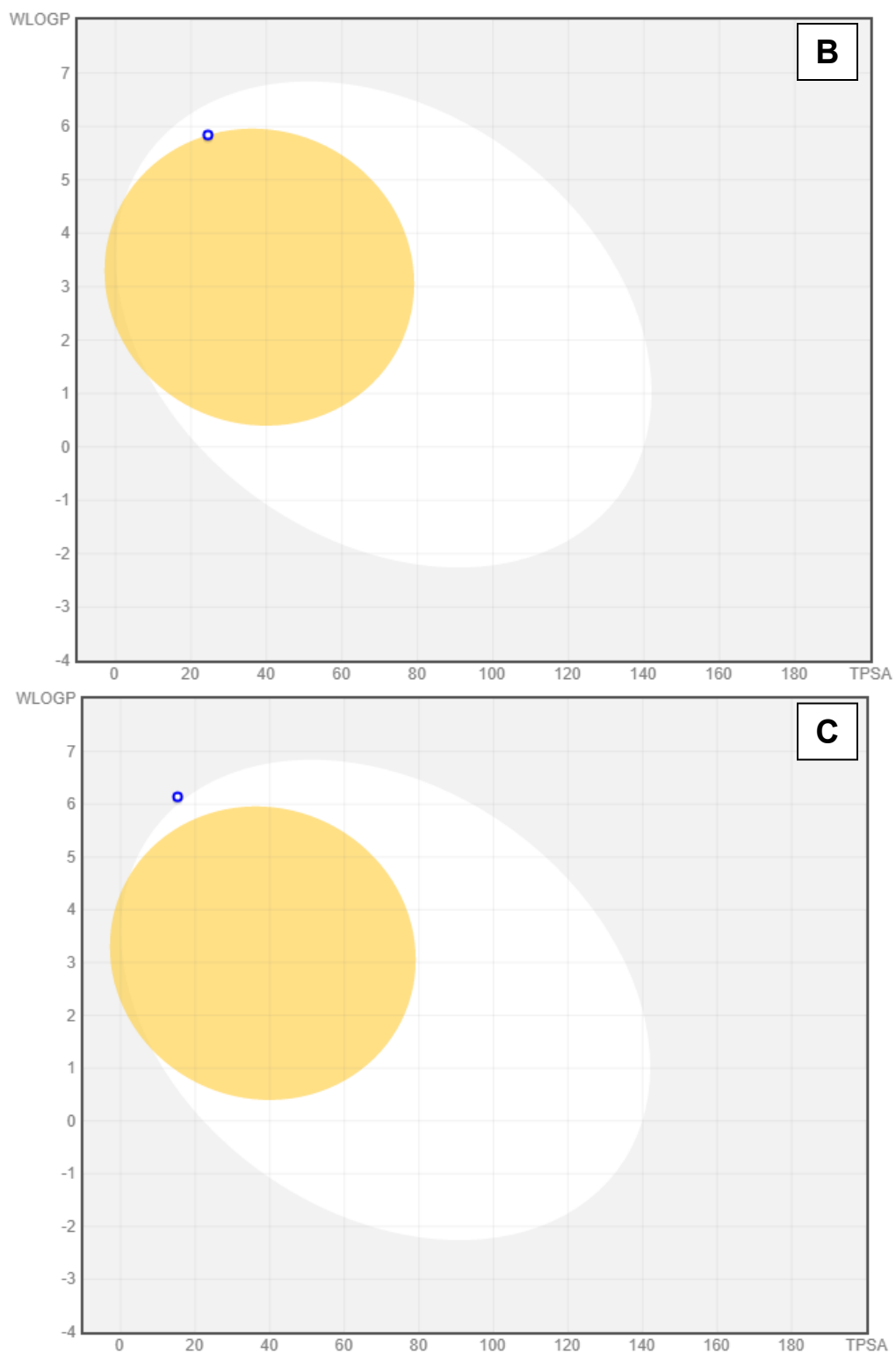
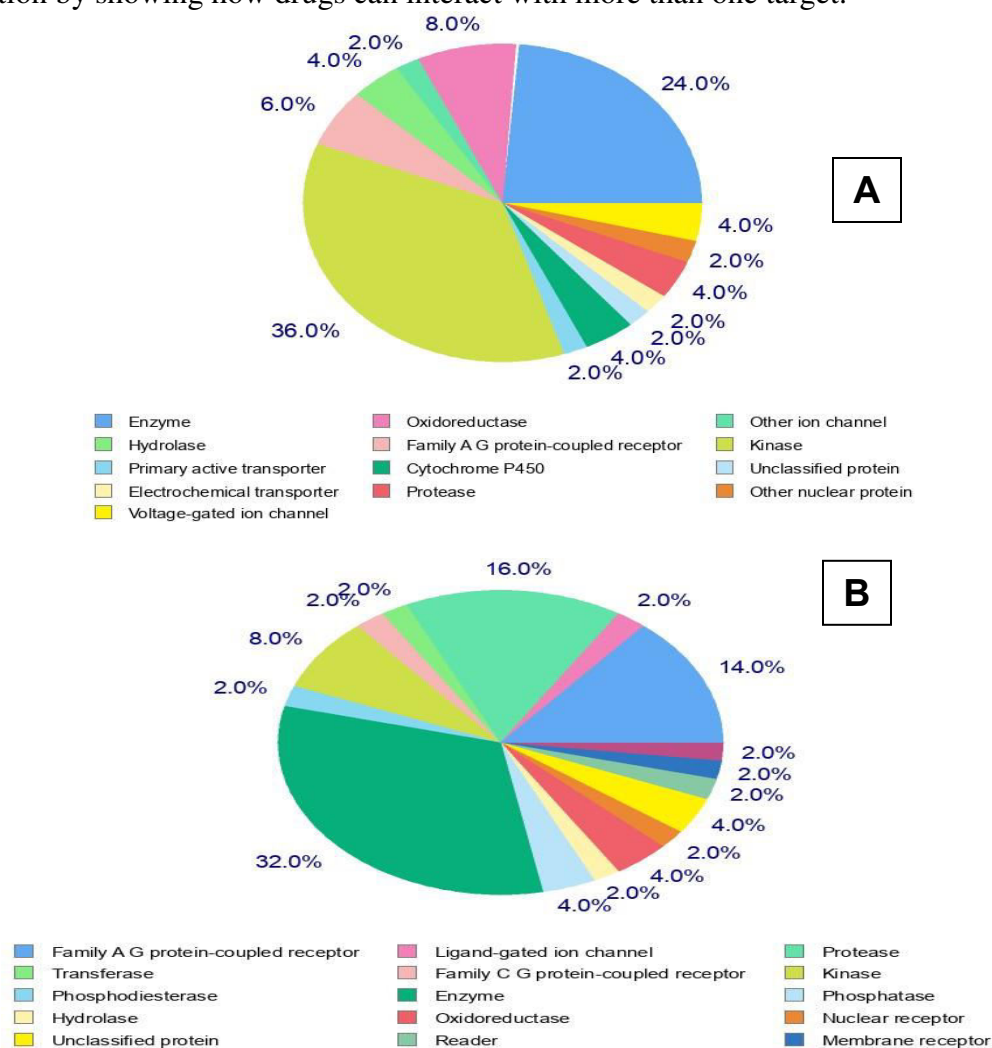


**Figure 4.**Boiled Egg Plot (A) Compound-1, (B)Compound-2, and (C) Compound-3.

### 3.4. Drug target identification

#### 3.4.1. Compound-1

Because the study is about reusing drugs, it is still very important to find the likely medicinal targets that Compound-1 can block with micromolar doses. The human (*Homo sapiens*), rat (*Rattus norvegicus*), and mouse (*Mus musculus*) models showed that compound-1 could block a number of targets, including an enzyme, an oxidoreductase, a transferase, a voltage-gated ion channel, a primary active transporter, a ligand-gated ion channel, and more (Figure 5). As expected, the results strongly backed the idea of using a semi-synthesized natural product to fight inflammation by showing how drugs can interact with more than one target.



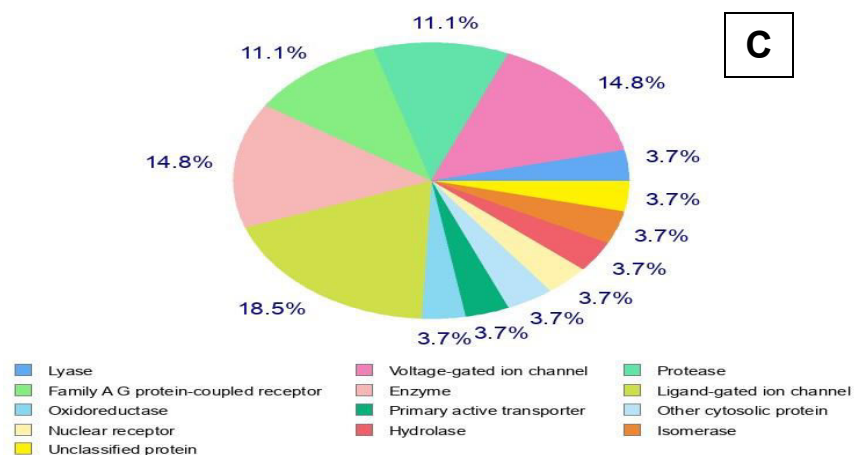
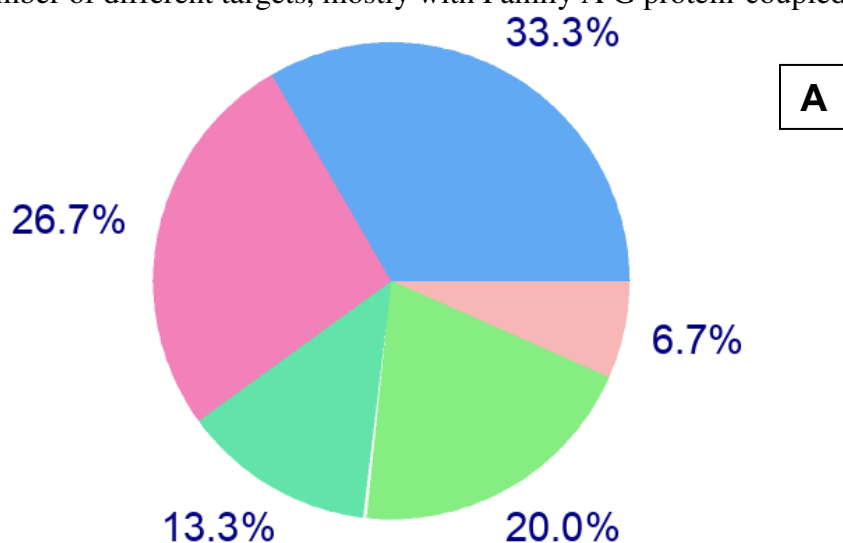


**Figure 5.** Predicted therapeutic targets of Compound-1 against (A) Human, (B) Mouse, and (C) Rat.

### 3.4.2. Compound-2

The study's main goal is to find out how Compound-2 interacts with therapeutic targets that are very important from a pharmacological point of view. It is still very important to precisely quantify the therapeutic targets that Compound-2 can ideally block at micromolar concentrations.

The Homo sapiens model showed that Compound-2 can block targets like the Family A G protein-coupled receptor (33.3%), Kinase (26.7%), Electrochemical transporter (13.3%), Protease (20%), and Hydrolase (6.7%) (Figure 6). It was shown that Compound-2 can block Family A G protein-coupled receptor (53.3%), Kinase (6.7%), Electrochemical transporter (6.7%), Unclassified protein (6.7%), Protease (20%), and Enzymes (6.7%). This was shown in a mouse model called *Mus musculus*. *Rattus norvegicus* was used as a model to show how Compound-2 works to block Family A G protein-coupled receptors (33.3%), Ligand-gated ion channels (20%), Voltage-gated ion channels (6.7%), Electrochemical transporters (6.7%), enzymes (6.7%), kinases (6.7%), and hydrolases (6.7%). The expected results strongly backed the idea that this small chemical could be used to treat colon cancer by showing that it could interact with a number of different targets, mostly with Family A G protein-coupled receptors.



**Family A G protein-coupled receptor (33.3%), Kinase (26.7%), Electrochemical transporter (13.3%), Protease (20%), Hydrolase (6.7%)**

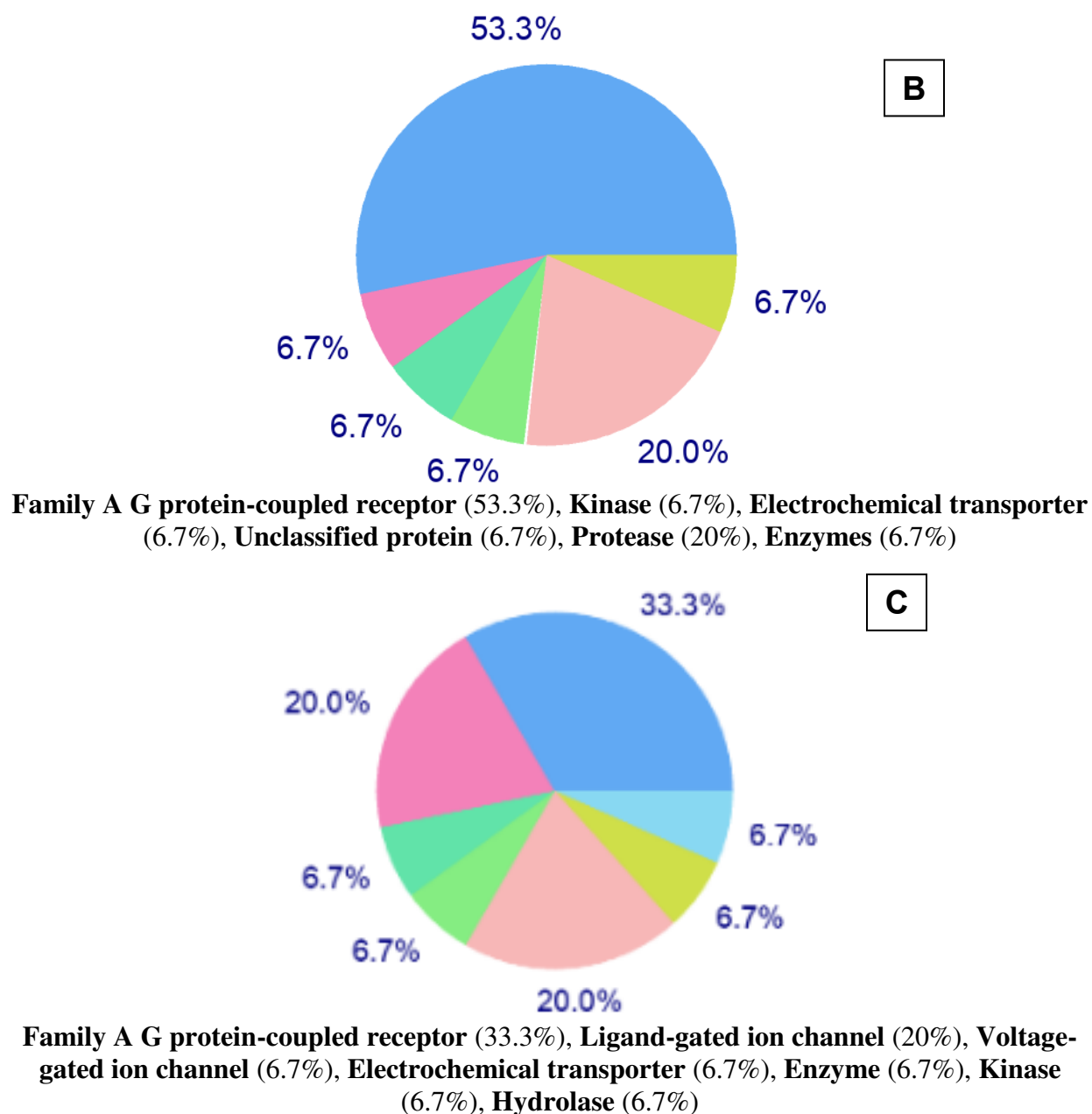


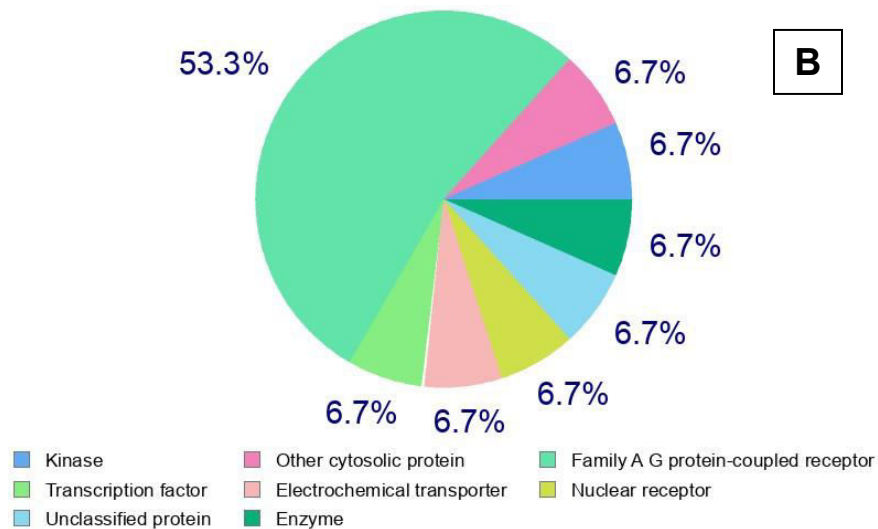
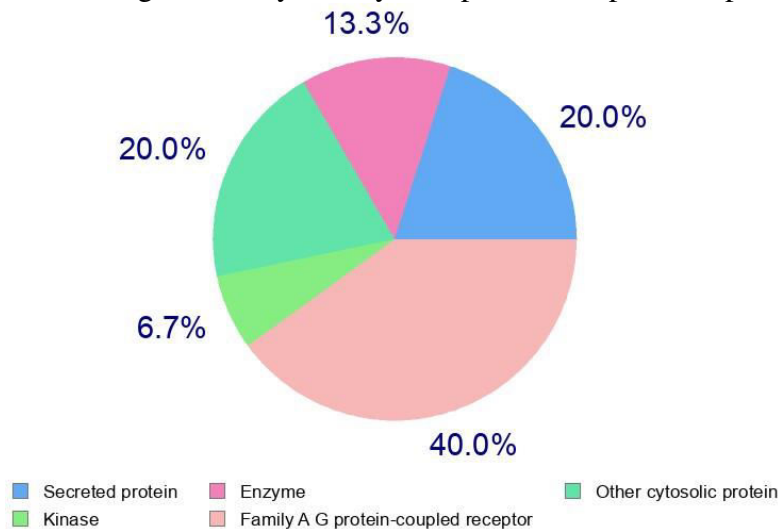
**Figure 6.** Predicted therapeutic targets of Compound-2 against (A) Human, (B) Mouse, and (C) Rat.

### 3.4.3. Compound-3

The study's main goal is to find out how Compound-3 interacts with therapeutic targets that are very important from a pharmacological point of view. It is still very important to precisely quantify the therapeutic targets that Compound-3 can ideally block at micromolar concentrations. People (*Homo sapiens*) were used as a model to show that Compound-3 can block Family A G protein-coupled receptors (40%), released proteins (20%), other cytosolic proteins (20%), enzymes (13.3%), and kinases (6.7%). It was shown that Compound-3 can block targets like the

Family A G protein-coupled receptor (40%), kinase (6.7%), enzymes (6.7%), nuclear receptor (6.7%), transcription factor (6.7%), unclassified protein (6.7%), electrochemical transporter (6.7%), and other cytosolic protein (6.7%). The mouse model was used to test this.

*Rattus norvegicus* was used as a model to show how Compound-3 works to block Family A G protein-coupled receptors (40%), enzymes (13.3%), voltage-gated ion channels (6.7%), ligand-gated ion channels (6.7%), kinases (6.7%), nuclear receptors (6.7%), and unclassified proteins (6.7%) (Figure 7). It was expected that the results would strongly support the idea that this small chemical could be used to fight inflammation by showing that it could interact with a number of different targets, mostly Family A G protein-coupled receptors.



**C**

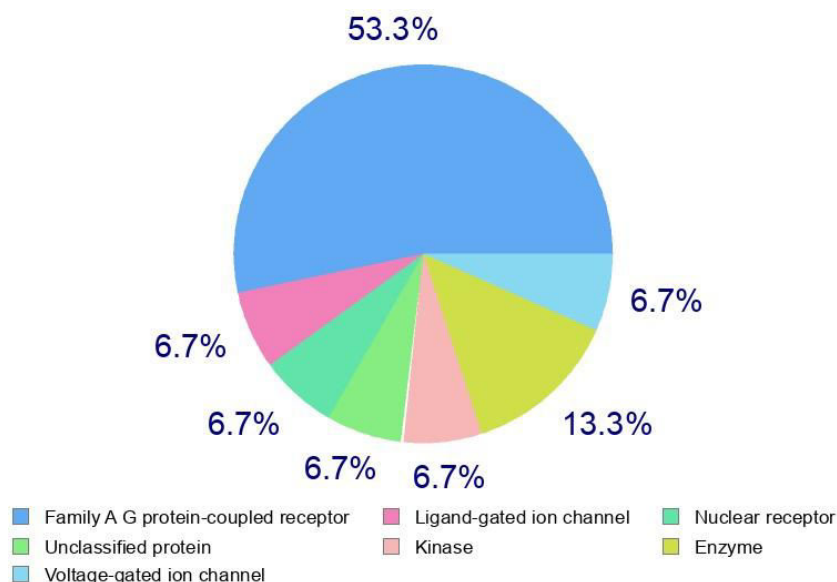


**Figure 7.** Predicted therapeutic targets of Compound-3 against (A) Human, (B) Mouse, and (C) Rat.

### 3.5. Degradation pathways for molecules

A pathway tree analysis predicts the sequential biochemical reactions that Yakuchinone B might undergo, leading to its breakdown into simpler molecules. This approach combines known enzymatic reactions and metabolic pathways commonly involved in the degradation of similar compounds. The degradation of Yakuchinone B is likely initiated by hydroxylation, a common metabolic transformation that introduces hydroxyl groups into the molecule. Cytochrome P450 enzymes, which are abundant in the liver, typically mediate this reaction. The initial hydroxylation could occur at the aromatic ring, resulting in the formation of a hydroxylated intermediate (**Figure 8**).

Following hydroxylation, the molecule may undergo further hydroxylation to form a catechol structure (adjacent dihydroxyl groups on the aromatic ring). This step enhances the molecule's solubility and prepares it for further metabolic processing. The catechol intermediate can undergo O-methylation, where one or both hydroxyl groups are methylated by catechol-O-methyltransferase (COMT). This step converts the dihydroxyl groups into methoxy groups, forming methoxy derivatives. The methoxy derivatives or the remaining hydroxyl groups can further undergo conjugation reactions such as glucuronidation or sulfation. These reactions enhance the solubility and facilitate the excretion of the compound from the body (**Figure 9**).

Enzymatic cleavage of the aromatic rings can occur, leading to the breakdown of the structure into smaller, more manageable fragments. This step is typically mediated by dioxygenases that cleave the aromatic ring between hydroxylated carbons, resulting in ring-opened products. The side chains of Yakuchinone B can undergo beta-oxidation, a process commonly associated with fatty acid degradation. This step reduces the length of the aliphatic chains, producing acetyl-CoA and shorter carboxylic acids. The final breakdown products of Yakuchinone B are typically small organic acids, alcohols, and CO<sub>2</sub>, which are easily excreted from the body. The conjugated metabolites, such as glucuronides and sulfates, are excreted via urine or bile (**Figure 10**).

### 3.5.1. Compound-1

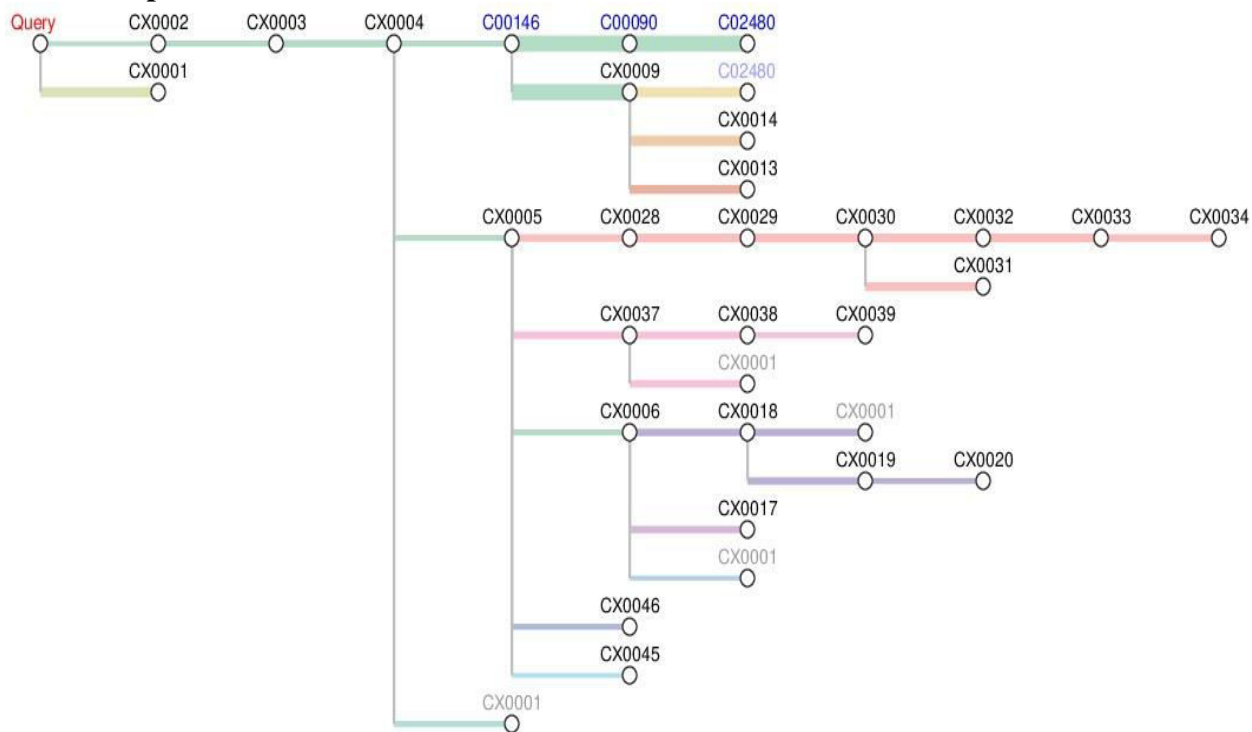


**Figure 8.** Predicted Pathway Tree for Compound-1.

### 3.5.2. Compound-2

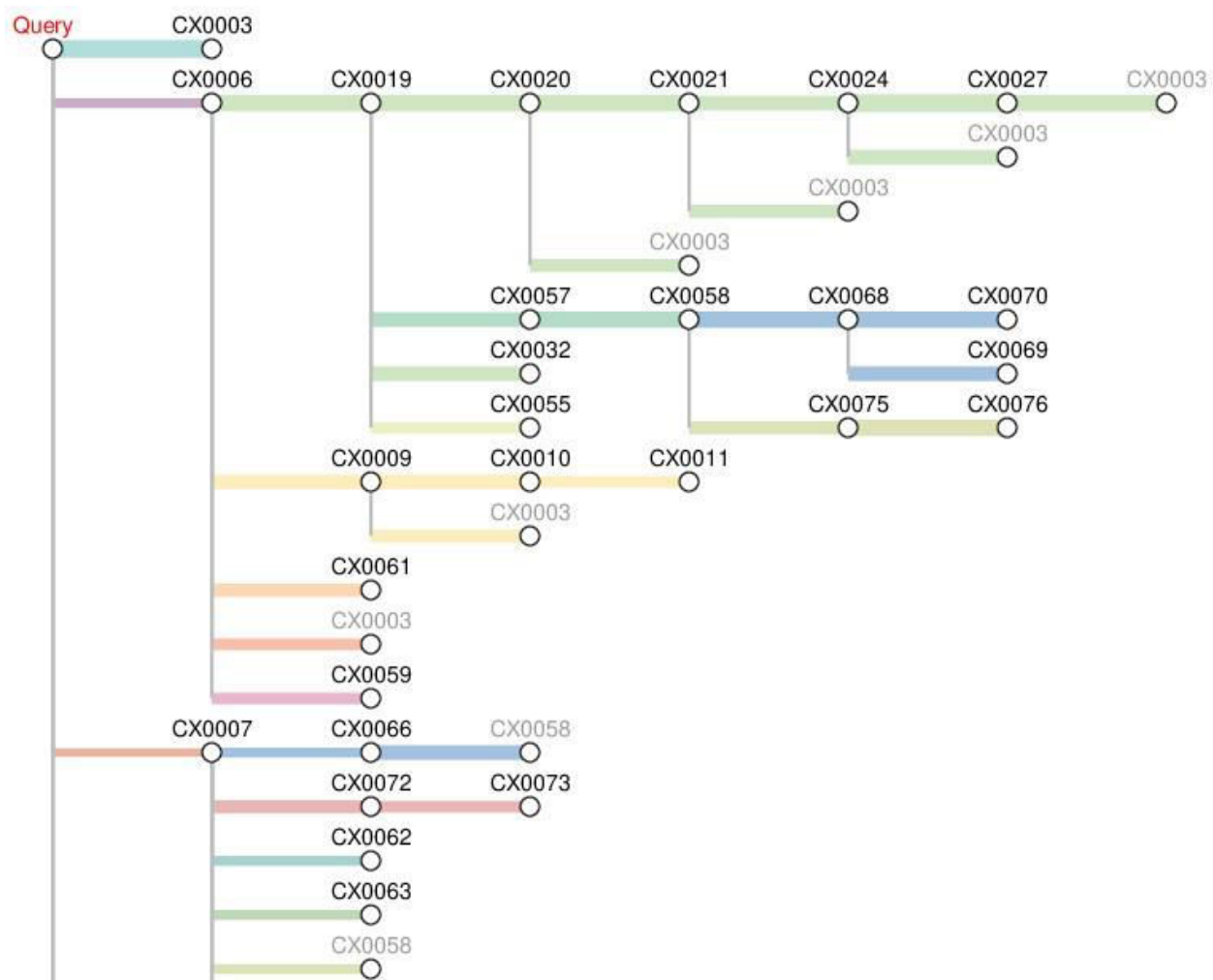


**Figure 9.** Predicted Pathway Tree for Compound-2.

### 3.5.3. Compound-3



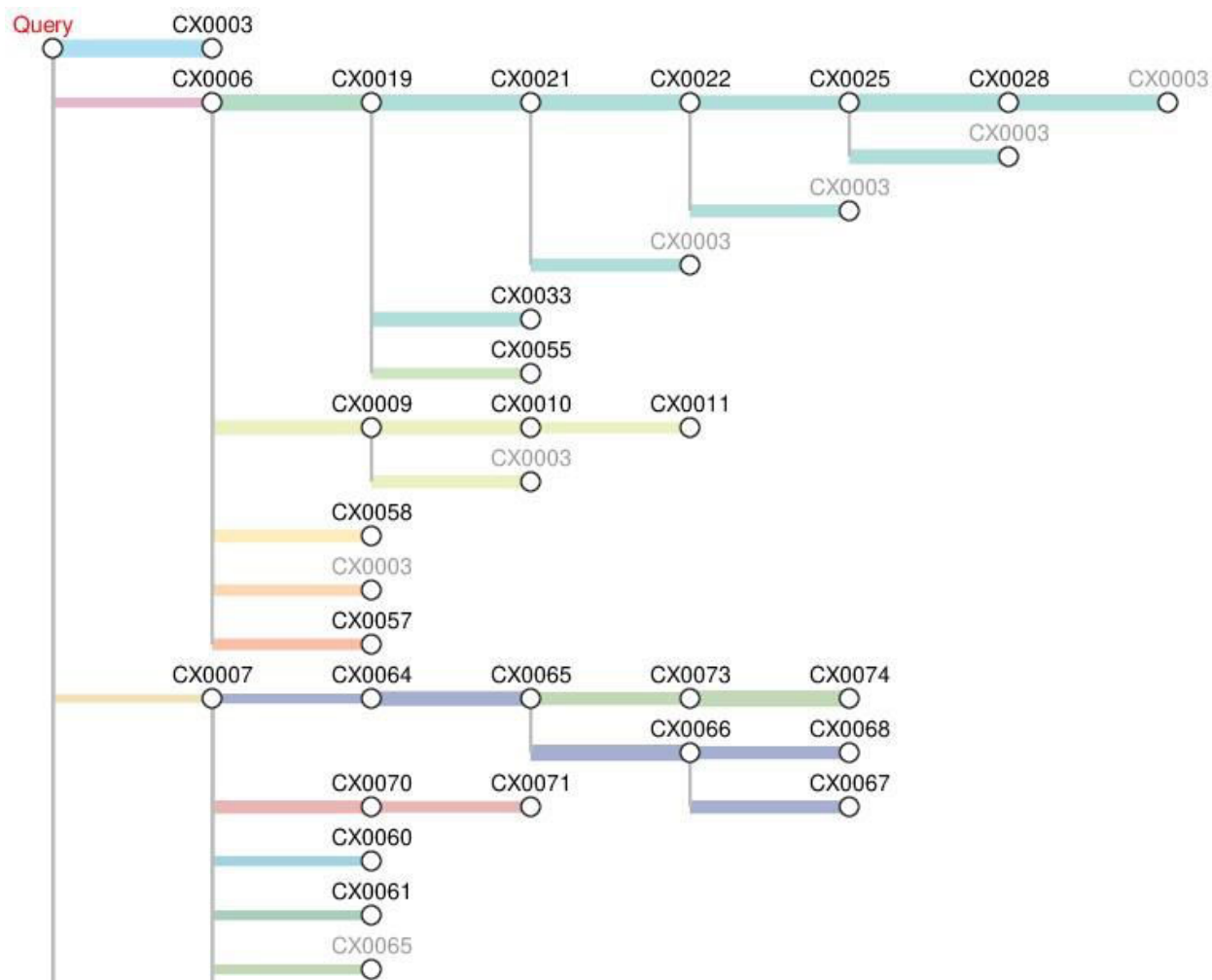


**Figure 10.** Predicted Pathway Tree for Compound-3.

### 3.7. Molecular Docking

The structure of novel Yakuchinone B derivative was sent for induced fit docking study by using Glide software and this docking result confirms that our compound has anti-inflammatory activity. The induced fit molecular docking studies confirmed the interaction of the Compound-3 scaffold with the inflammatory mediator COX-1, COX-2, LOX-5, and TXA-2. The result of Compound-3 for COX-1 inhibitory potential and PLA-2 inhibitory potential are more promising. The Compound-3 displayed a notable glide score for COX-1, COX-2, and PLA-2. The Compound-3 displayed notable Glide scores of -8.62 Kcal/mol for COX-1 and exhibited interaction through hydrogen bonding with GLYB45 residue. For COX-2, the Compound-3 displayed notable Glide scores of -6.61 Kcal/mol and exhibited interaction through pi-alkyl bonding with LYS454 and ARG29 residues. The Compound-3 displayed notable Glide scores of -6.15 Kcal/mol for LOX-5 and exhibited interaction through pi-alkyl bonding with LYS196, TRPA198, and LEUA154 as well hydrogen bonding with TRPA198 residue. The Compound-3 displayed notable Glide scores of -5.34 Kcal/mol for TXA-2 and exhibited interaction through pi-alkyl bonding with VALA111, LEUA161, and VALA110, TRPA157, and LEUA76 as well pi-pi bonding with PHEA107 residue and pi-sulfur bonding with PHEA114 residue (**Table 2**).

**Table 2.** Glide scores of Compound-3 as inflammatory enzymes inhibitor.

| S. No. | Compound | Energy (Kcal/mol) |
|--------|----------|-------------------|
| 1.     | COX-1    | -8.62             |
| 2.     | COX-2    | -6.61             |
| 3.     | LOX-5    | -6.15             |
| 4.     | TXA-2    | -5.34             |

### 3.7.1. COX-1 inhibitory potential

The induced fit molecular docking studies confirmed the interaction of the synthesized Schiff base scaffold with the inflammatory mediator COX-1. The Schiff base displayed notable Glide scores of -8.62Kcal/mol and exhibited interaction through hydrogen bonding with GLY B45 residue and pi-alkyl bonding with PRO B130, LEU B152, CYS B47, VAL B48, and ILE B46(Figure 11).

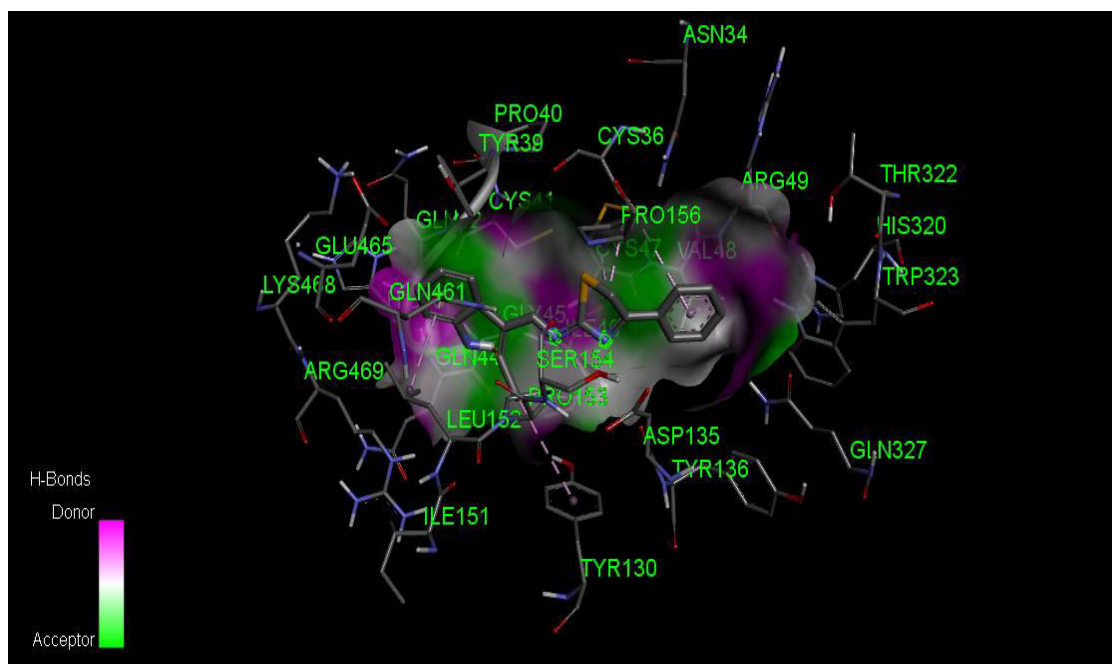


**Figure 11.** 3D binding modes and interactions of the synthesized compound with COX-1 enzyme.

### 3.7.2. COX-2 inhibitory potential

The induced fit molecular docking studies confirmed the interaction of the synthesized Schiff base scaffold with the inflammatory mediator COX-2. The Schiff base displayed notable Glide scores of -6.61 Kcal/mol and it exhibited interaction through alkyl bonding with ARG D:29 and LYS D:454(Figure 12).

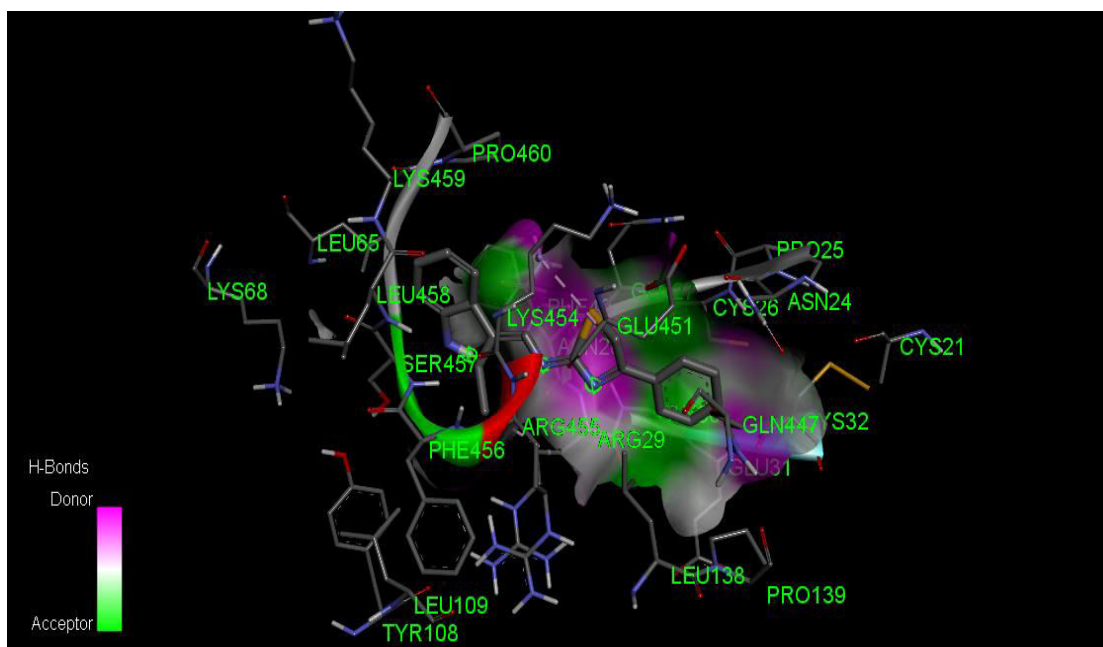


**Figure 12.3D** binding modes and interactions of the synthesized compound with COX-2 enzyme.

### 3.7.3. LOX-5 inhibitory potential

The Schiff base displayed notable Glide scores of -6.15 Kcal/mol and exhibited interaction through pi-alkyl bonding with LYS A196, TRP A198, and LEU A154 as well hydrogen bonding with TRP A198 residue(**Figure 13**).

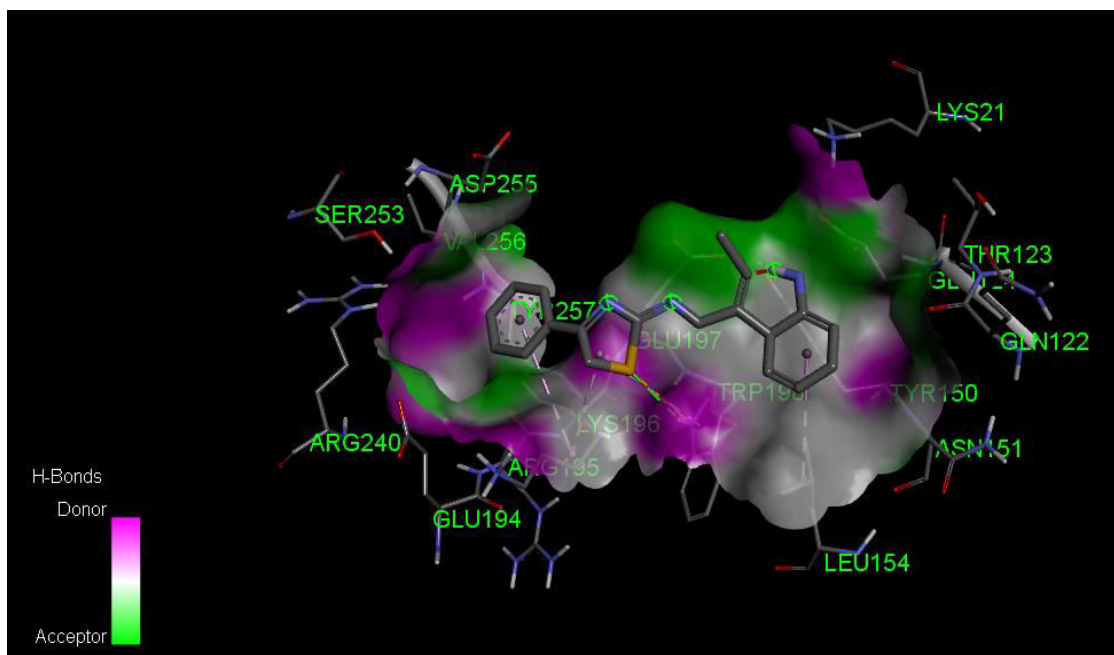


**Figure 13.3D** binding modes and interactions of the synthesized compound with LOX-5 enzyme.

### 3.7.4. TXA-2 inhibitory potential

The Schiff base displayed notable Glide scores of  $-5.34$  Kcal/mol and exhibited interaction through pi-alkyl bonding with VAL A111, LEU A161, VAL A110, TRP A157, and LEU A76 as well pi-pi bonding with PHE A107 residue and pi-sulfur bonding with PHE A114 residue (Figure 14).

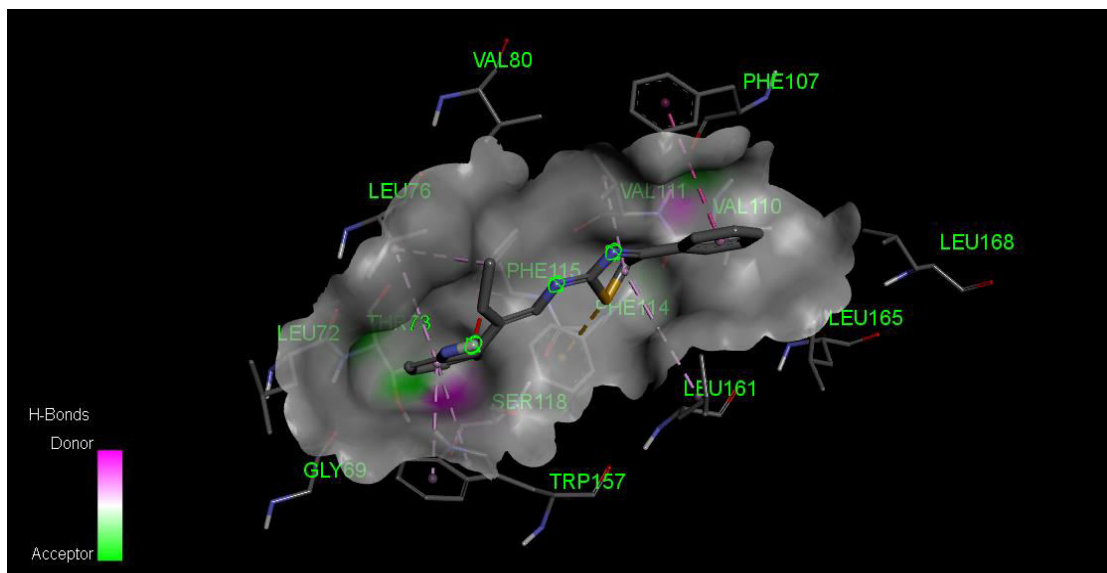


**Figure 14.** 3D binding modes and interactions of the synthesized compound with TXA-2enzyme.

The study provided directions towards the rational development of anti-inflammatory agents by deciphering the essential structural requirements and substituents for modulation. The position and the number of hydrogen group were found to be a necessary aspect of designing better inhibitors.

### 3.8. Molecular Simulations

Molecular dynamics models (MDS) help us understand how protein-ligand groups move, change shape, stay stable, and other things when they interact with medical chemicals that cause proteins to go through big conformational changes. A 100 ns MD computer study of all the atoms was used to look into how the Yakuchinone B derivative (Compound 3) moved inside COX-1.

A bunch of parameters were calculated from the full MD simulations to look at how the ligand binds to the main protease protein and how it moves and changes over time. These parameters included the protein  $C\alpha$  atoms Root Mean Square Deviation (RMSD), the ligand RMSD with respect to the protein, the ligand Root Mean Square fluctuation (RMSF), and the protein-ligand contact analysis. The RMSD value from the MD track can explain why the protein  $C\pm$  atoms that are connected to drug molecules are moving apart. The RMSD plots against modelling time are shown in Figure 15A. Small changes mean that a stable conformation has been reached, and vice versa. For the first 18 ns, it showed that the complex RMSD changed between  $2.1\text{\AA}$  and  $2.7\text{\AA}$ . After that, it stayed stable and had a mean value of  $2.2\text{\AA}$  for the rest of the experiment. Because of equilibration, the ligand RMSDs changed a lot, reaching a high point of  $4.2\text{\AA}$  in the first 10 ns. After that, the interactions became more stable and stayed that way for the rest of the run.

Figure 15B shows the RMSF curve of each amino acid residue as a function of the amount of residues. This is used to figure out how mobile the complex is. A high RMSF value means that the structure of the protein is flexible, there are loose bonds, or loops are present. A low value,

on the other hand, means that the structure is stable and secondary structures like sheets and helices are present. The residues that change the most during the exercise are shown by the peak in this picture. The changes started at 0.5Å and went up to 2.5Å. The -C and -N ends saw the most changes. In this mixture, the Yakuchinone B derivative (Compound 3) interacted with 21 amino acids of the COX-1 protein. These included Thr24 (1.05Å), Thr25 (0.757Å), Cys44 (0.768Å), Thr45 (1.272Å), Ser46 (1.262Å), Met49 (0.932Å), Asn142 (0.928Å), Cys145 (0.492Å), Tyr154 (1.172Å), Met165 (0.602Å), Glu166 (0.644Å), Leu167 (0.714Å), Pro168 (1.146Å), Arg188 (0.834Å), Gln189 (1.143Å), Thr190 (1.156Å), Ala191 (1.514Å), Gln192 (1.097Å), Pro252 (1.067Å), Ala255 (1.141Å), and Gln256 (1.171Å). The low numbers that were found probably meant that none of the amino acid sites changed a lot during the exercise. Compound 3 is a product of Yakuchinone B. The polar terminal hydroxyl connected with Gln192 and Thr190 through direct hydrogen bonding and amino acid-mediated hydrogen bonding, respectively. In the same way, Gln189 and Ser46 form hydrogen bonds with the terminal ester group's carbonyl oxygen at 15% and 16% of the simulation time, respectively. Having a lot of interactions between molecules is very important for the security of a ligand-protein complex. The picture above shows that these exchanges can be grouped and summed up by type. There are four different kinds of interactions between proteins and ligands: hydrogen bonds, hydrophobic interactions, ionic interactions, and water bridges. Throughout the journey, the stacked bar charts are normalised. For example, a number of 0.5 means that the exact touch is kept 50% of the time during the exercise. It is possible to get values higher than 1.0 because the same type of ligand can interact with more than one protein residue. In this complex, Met165 interacts with water most of the time, which is 70% of the modelling time (Figure 15C). RMSD, RMSF, and protein-ligand contact analysis parameters from the MD simulation track showed that the protein-ligand complex stayed stable in changing states, and the COX-1 protein inhibitor that was suggested was kept inside the receptor cavity.

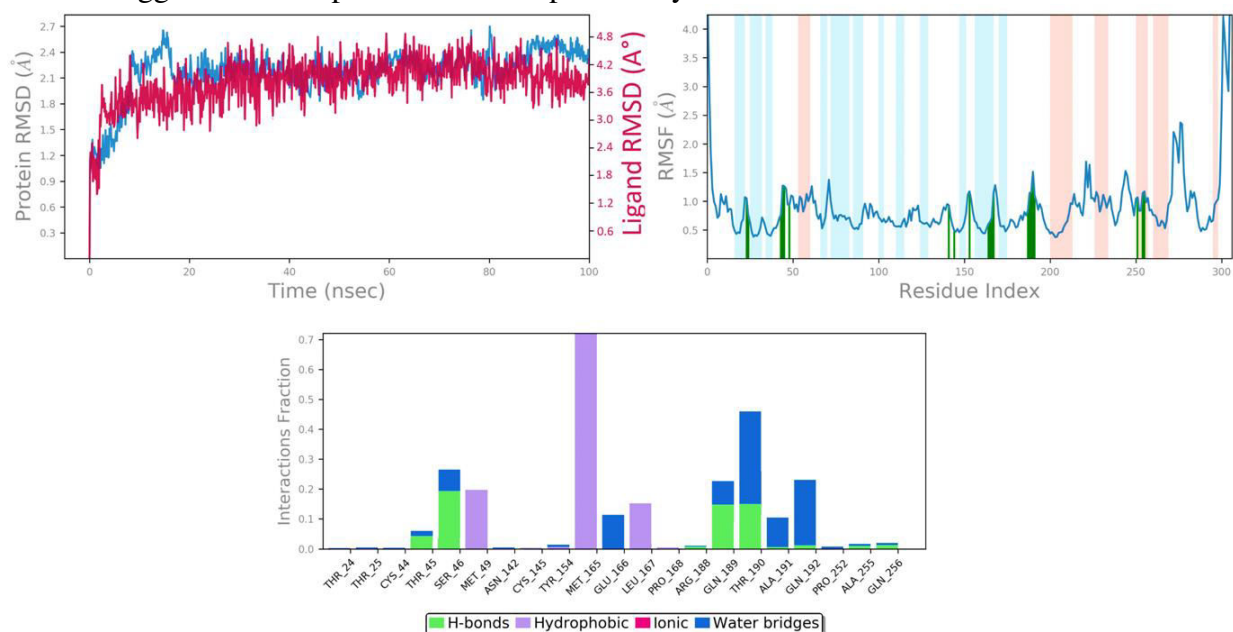


**Figure 15.** MD simulation analysis of Yakuchinone B derivative (Compound 3) in complex with COX-1 (A) RMSD (Protein RMSD is shown in grey while RMSD of compound Yakuchinone B derivative (Compound 3) are shown in red) (B) Protein RMSF, and (C) Protein–ligand contact analysis of MD trajectory.



### 3.9. Physical characterization of novel Yakuchinone B derivatives

#### 3.9.1. Appearance

The final compound was found to be solid, white in color, and crystalline in nature (Table 3).

**Table 3.** Characterization of novel Yakuchinone B derivatives.

| Characteristics    | Compound-1              | Compound-2             | Compound-3               |
|--------------------|-------------------------|------------------------|--------------------------|
| Appearance         | White crystalline solid | Yellow amorphous solid | Yellow crystalline solid |
| Yield (%)          | 64.55                   | 73.62                  | 81.23                    |
| Melting point (°C) | 218-219                 | 159-161                | 181-182                  |
| Rf value           | 0.54                    | 0.43                   | 0.77                     |

#### 3.9.2. Yield

The compounds (1-3) were observed to be marginal (64%), moderate (73%), and 81% (significant), respectively. On consecutive purification through column chromatography, the purity of the products were ascertained, however, the quantity was less.

#### 3.9.3. Melting point

Through digital melting point apparatus, the melting point of the compounds (1-3) was detected to be 218-219°C, 159-161°C, and 181-182°C. This study revealed the conversion of intermediate product into the compounds.

#### 3.9.4. Rf value

Using the mobile phase composition of acetonitrile: ethylacetate (6:4 v/v), the Rf values of the final compound was observed to be 0.54 (for compound-1), 0.43 (for compound-2), and 0.77 (for compound-3) (Figure 16). This study revealed the successful formation of all the novel Yakuchinone B derivatives.

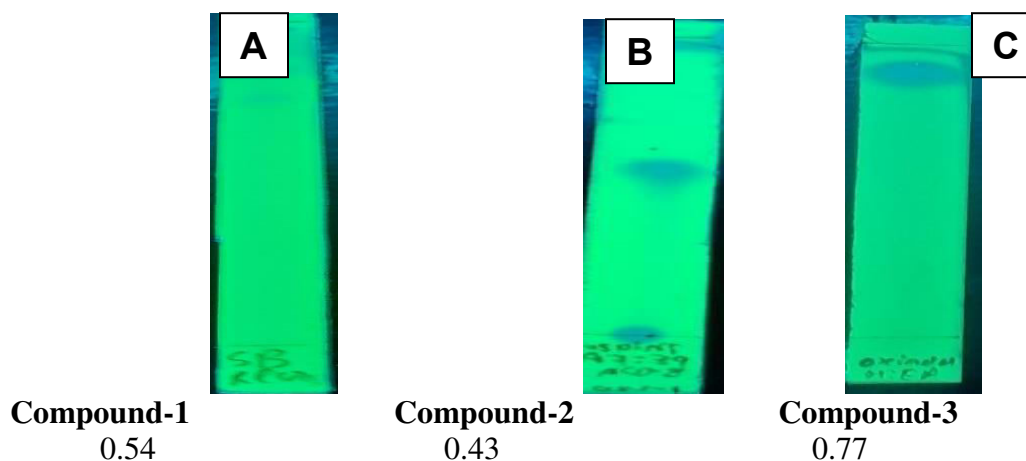
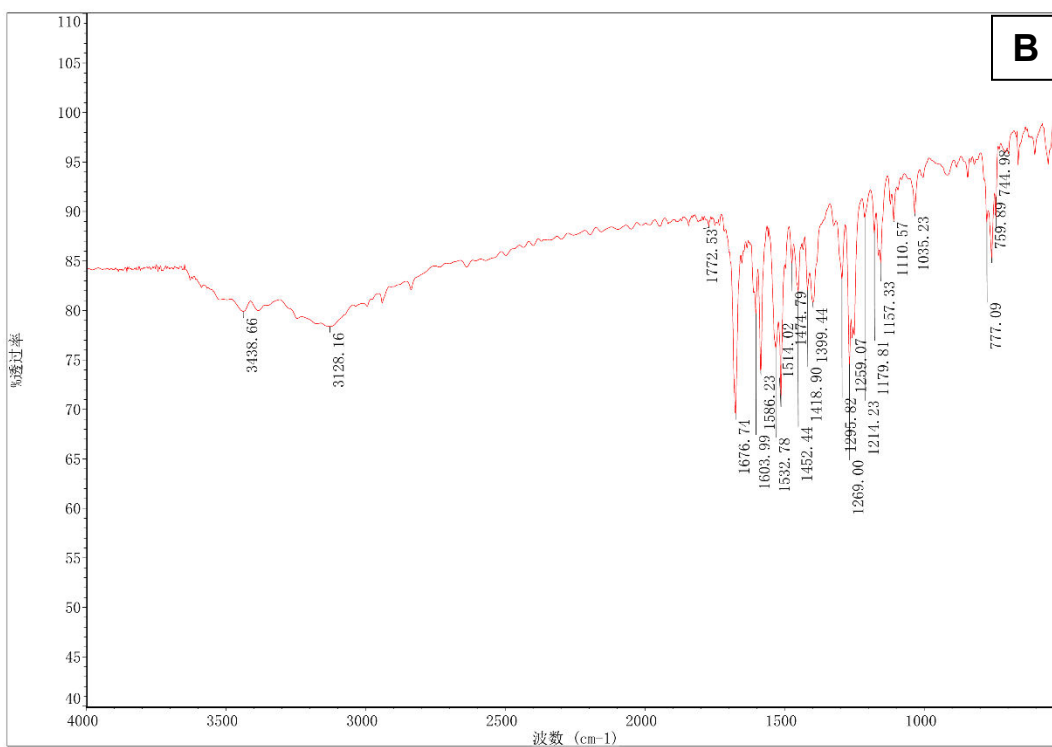
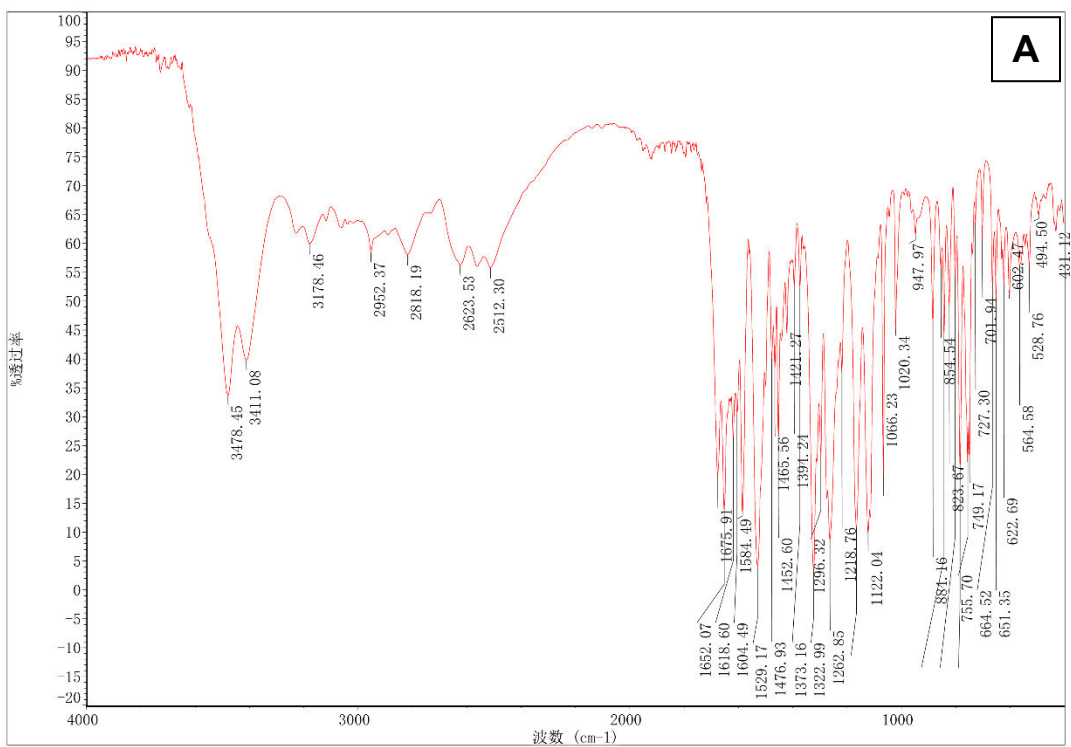


**Figure 16.** Chromatogram of novel Yakuchinone B derivatives (A) Compound-1, (B) Compound-2, and (C) Compound-3.

### 3.10. Spectroscopic characterization of final compound

#### 3.10.1. FTIR Spectroscopy

The spectroscopy study supported the formation of the compound. The disappearance of (-Cl) component ( $655\text{ cm}^{-1}$ ) and the appearance of NH at  $3274\text{ cm}^{-1}$  confirmed the formation of the novel Yakuchinone B derivative. The C-N component at  $1701\text{ cm}^{-1}$  substantiates the presence of the newly added six-membered portion to the parent molecule (**Figure 17**).



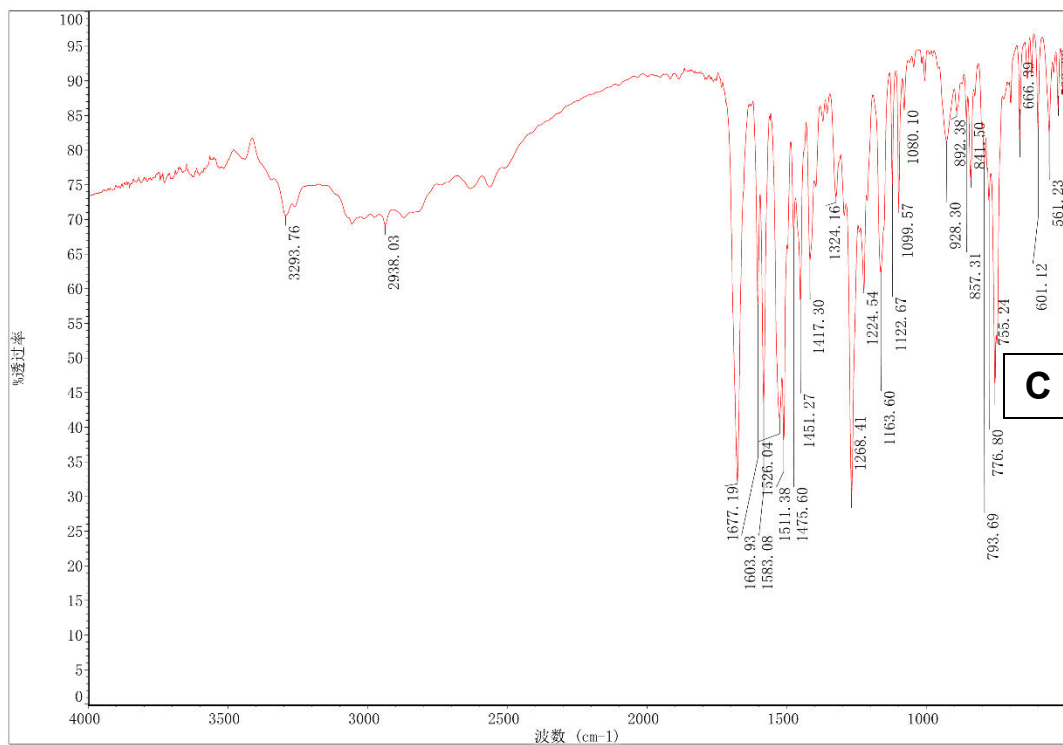


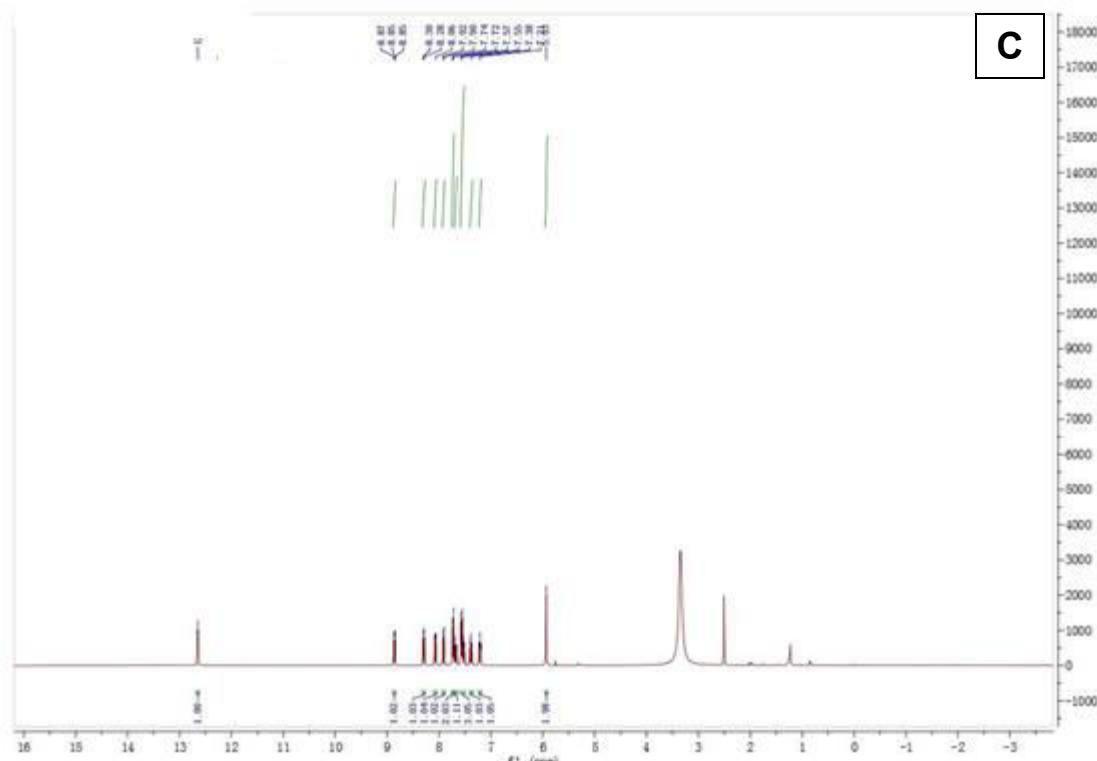
**Figure 17.** FTIR spectrum of novel Yakuchinone B derivatives (A) Compound-1, (B)Compound-2, and (C) Compound-3.

### 3.10.2. <sup>1</sup>H-NMR Spectroscopy

The <sup>1</sup>H-NMR readings showed a few important things. The range of 7.0 to 8.0 ppm in the spectrum makes the protons in the molecule stand out. The –NH and –OH parts were also found at 10.4 ppm and 3.39 ppm, respectively. (**Figure 18**).



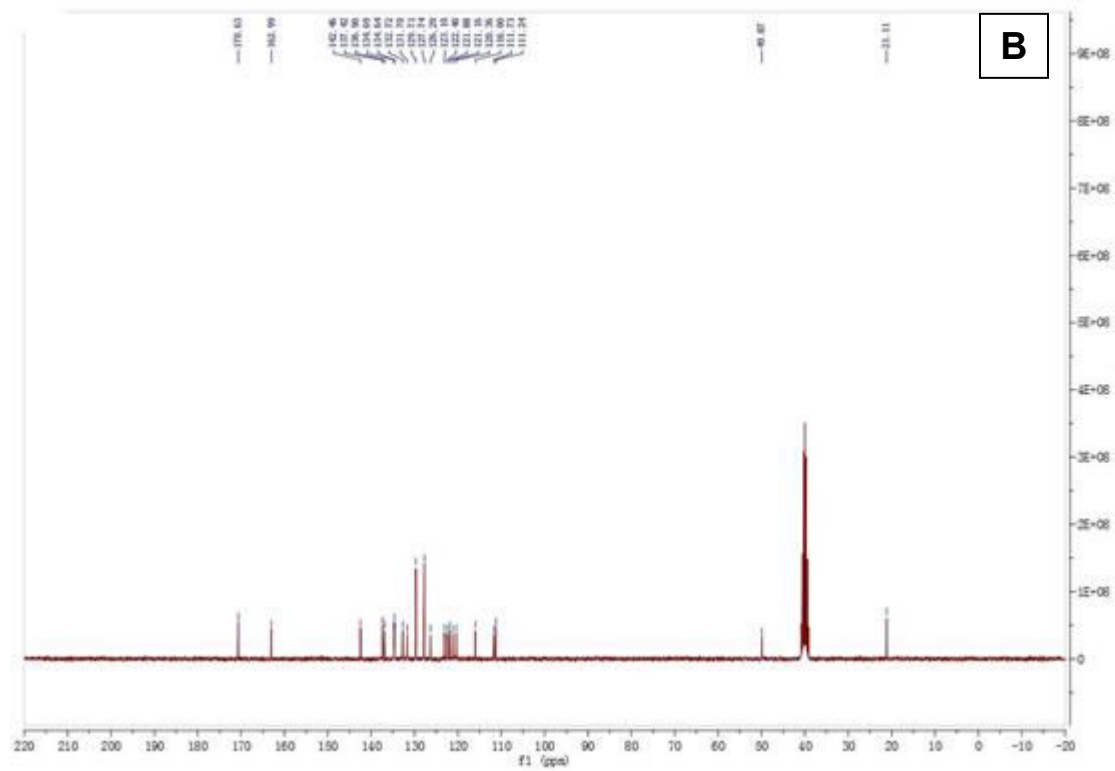
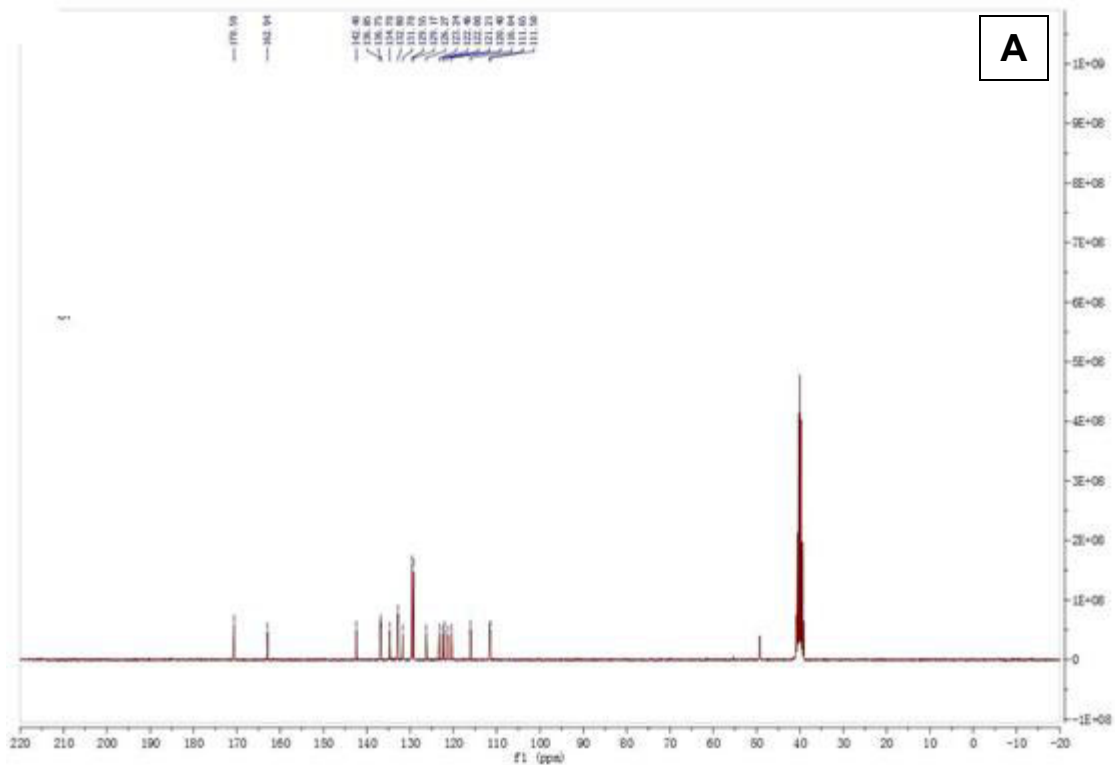




**Figure 18.**  $^1\text{H-NMR}$  of novel Yakuchinone B derivatives (A) Compound-1, (B)Compound-2, and (C) Compound-3.

### 3.10.3. $^{13}\text{C-NMR}$ Spectroscopy

The  $^{13}\text{C-NMR}$  spectrum also confirmed the formation of the novel derivative and showed analogous results to that of proton NMR. The spectral range of 120.0-140.0 ppm emphasizes the presence of protons in the compound. Additionally, the  $-\text{NH}$  and  $-\text{OH}$  aspects were located at 78.2 ppm and 39.6 ppm, respectively (**Figure 19**).





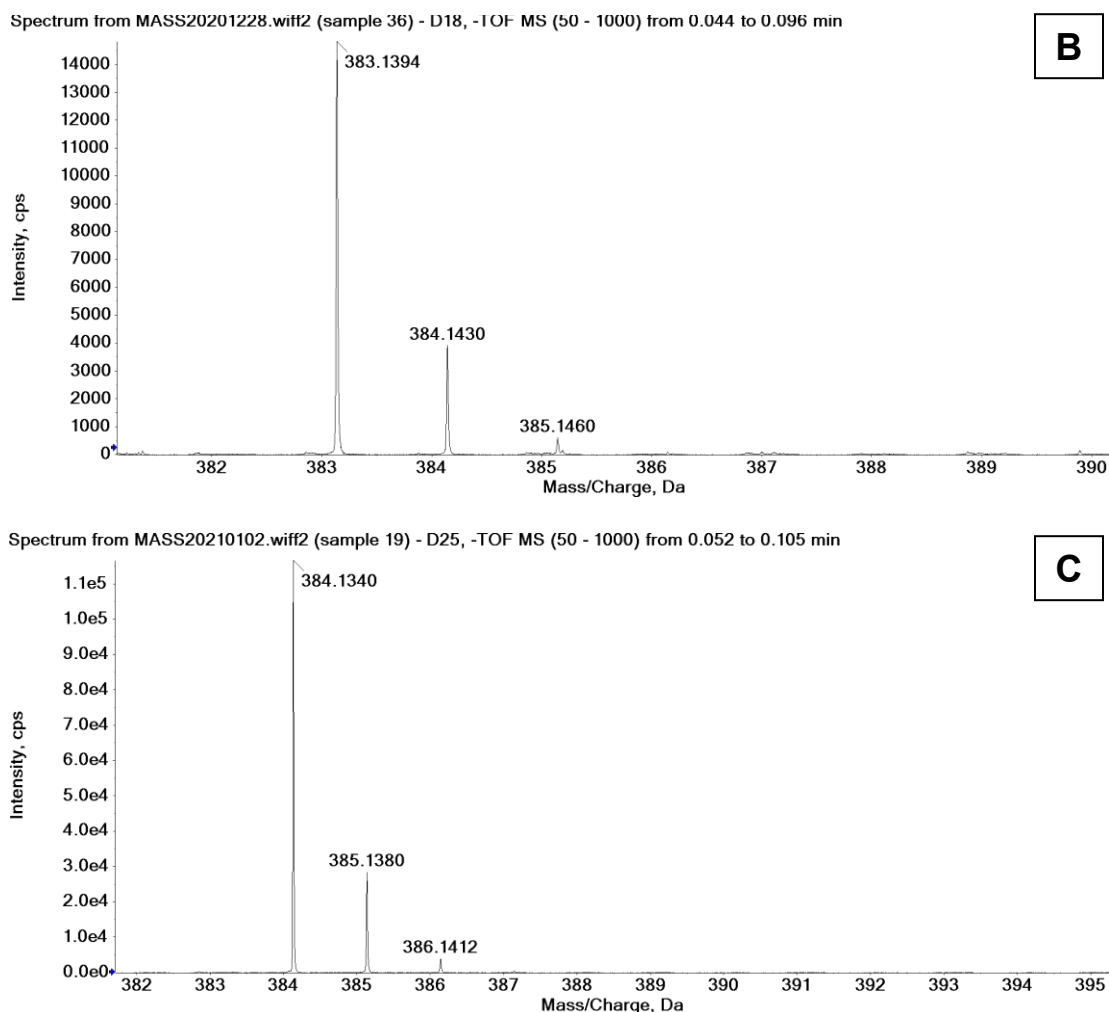


**Figure 20.** Mass spectra of novel Yakuchinone B derivatives (A) Compound-1, (B) Compound-2, and (C) Compound-3.

### 3.11. Anti-inflammatory study

The initial paw volume upto ankle joint of each group was measured using plethysmometer. Animal of group C, D, E, F were treated with the single dose of Ibuprofen, and dose ranges of Compound-3, respectively. An injection of 0.1 mL of newly made 1% w/v carrageenan suspension in normal saline into the left hind paw caused acute inflammation in all groups except group A after 30 minutes. Our team used a plethysmometer to measure the size of the paw oedema 1, 2, 3, 4, 8, and 12 hours after injecting carrageenan. The 30 mg/kg amount of Compound-3 (group-VI) had the biggest effect on reducing the size of the rat paw oedema compared to the control group. After 12 hours, the percentage of oedema reduction was  $86.31 \pm 2.49\%$ .

The average amount of paw oedema in each group was found and compared to the control group's. One-way ANOVA and the Dunnett test were used to find statistical significance. A value of less than 0.0001 was seen as statistically significant when the data was quite significant. The results of mean paw edema volume are shown in **Table 4** and % edema inhibitions are as shown in **Table 5**. Anti-inflammatory activity of different doses is as shown in **Figure 21**.

**Table 4.** Mean paw edema volume after oral dose of test groups and standard.

| S. No. | Groups                             | Mean paw edema volume after hour* |                        |                        |                        |                        |
|--------|------------------------------------|-----------------------------------|------------------------|------------------------|------------------------|------------------------|
|        |                                    | 1                                 | 2                      | 4                      | 8                      | 12                     |
| 1.     | Normal(Saline)                     | 0.18±0.1                          | 0.18±0.1               | 0.18±0.1               | 0.18±0.1               | 0.18±0.1               |
| 2.     | Carrageenan control(0.1 mL 1% w/v) | 0.88±0.05                         | 1.15±0.2               | 1.35±0.11              | 1.4±0.1                | 1.58±0.11              |
| 3.     | Standard (30 mg/kg)                | 0.73±0.05 <sup>b</sup>            | 0.71±0.05 <sup>a</sup> | 0.63±0.05 <sup>a</sup> | 0.48±0.11 <sup>a</sup> | 0.28±0.15 <sup>a</sup> |
| 4.     | Compound-1 (30 mg/kg)              | 0.71±0.05 <sup>b</sup>            | 0.63±0.1 <sup>a</sup>  | 0.58±0.05 <sup>a</sup> | 0.43±0.1 <sup>a</sup>  | 0.31±0.1 <sup>a</sup>  |
| 5.     | Compound-2 (30 mg/kg)              | 0.68±0.1 <sup>a</sup>             | 0.53±0.11 <sup>a</sup> | 0.51±0.05 <sup>a</sup> | 0.4±0.1 <sup>a</sup>   | 0.25±0.1 <sup>a</sup>  |
| 6.     | Compound-3 (30 mg/kg)              | 0.65±0.05 <sup>a</sup>            | 0.51±0.05 <sup>a</sup> | 0.43±0.05 <sup>a</sup> | 0.35±0.05 <sup>a</sup> | 0.21±0.05 <sup>a</sup> |

\*: Values represented as mean ± S.E.M. (n=6), <sup>a</sup>: P<0.0001 compared to control<sup>b</sup>: P<0.0003

**Table 5.** Percent edema inhibition after oral dose of test groups and standard compound.

| S. No. | Groups                              | % Edema Inhibition after hour <sup>#</sup> |                          |                         |                         |                         |
|--------|-------------------------------------|--|--------------------------|-------------------------|-------------------------|-------------------------|
|        |                                     | 1  | 2                        | 4                       | 8                       | 12                      |
| 1.     | Normal (Saline)                     | –  | –                        | –                       | –                       | –                       |
| 2.     | Carrageenan control (0.1 mL 1% w/v) | –  | –                        | –                       | –                       | –                       |
| 3.     | Standard (30 mg/kg)                 | 16.98±12.83                                | 37.68±12.61              | 53.08±8.93              | 65.47±10.74             | 82.10±10.01             |
| 4.     | Compound-1 (30 mg/kg)               | 18.86±6.56 <sup>c</sup>                    | 44.92±10.68 <sup>c</sup> | 56.79±8.93 <sup>c</sup> | 69.04±4.61 <sup>c</sup> | 80±4.84 <sup>c</sup>    |
| 5.     | Compound-2 (30 mg/kg)               | 22.64±13.70 <sup>c</sup>                   | 53.62±15.46 <sup>b</sup> | 61.72±3.82 <sup>c</sup> | 71.42±8.03 <sup>c</sup> | 84.21±7.46 <sup>c</sup> |
| 6.     | Compound-3 (30 mg/kg)               | 26.41±10.48 <sup>c</sup>                   | 55.07±5.64 <sup>a</sup>  | 67.90±1.37 <sup>a</sup> | 75±2.78 <sup>a</sup>    | 86.31±2.49 <sup>a</sup> |

<sup>#</sup>: Values represented as mean ± S.E.M. (n=6), <sup>a</sup>: P<0.009 compared to standard<sup>b</sup>: P<0.02, <sup>c</sup>: Not significant

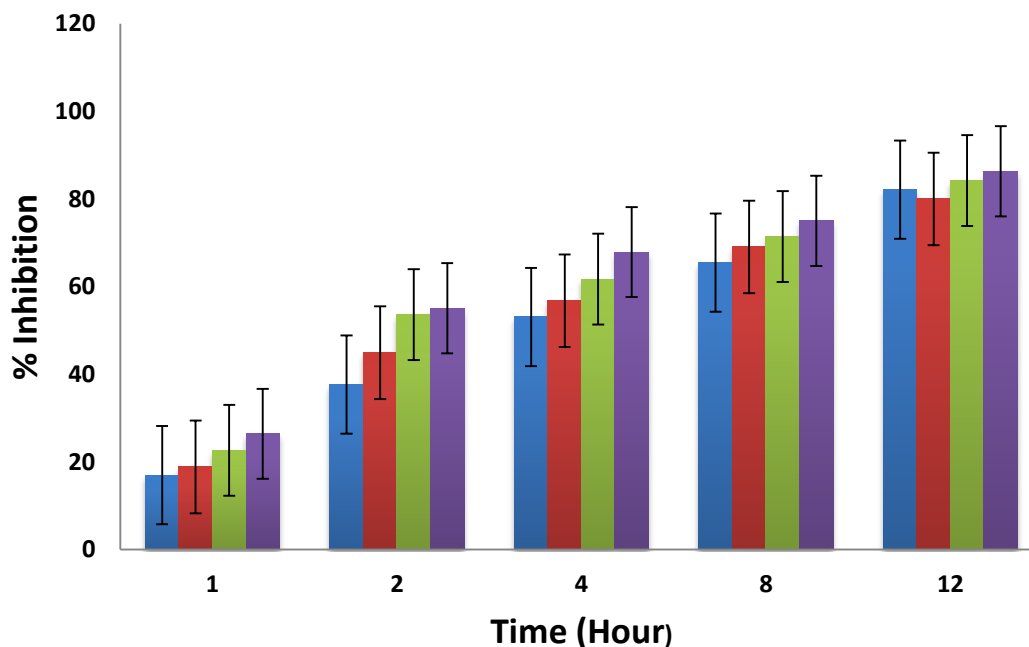


**Figure 21.** %Edema inhibition of novel Yakuchinone B derivatives.

#### 4. CONCLUSION

The study on the synthesis of novel derivatives of Yakuchinone B as promising anti-inflammatory agents has provided significant insights into the potential therapeutic applications of these compounds. This research has successfully demonstrated the feasibility of modifying the Yakuchinone B structure to enhance its anti-inflammatory properties, thereby laying the groundwork for the development of new, more effective treatments for inflammatory conditions. Through a combination of synthetic chemistry techniques and rigorous biological evaluation, several novel derivatives were designed and synthesized. These derivatives were systematically tested for their anti-inflammatory activity using established *in vitro* and *in vivo* models. The results consistently showed that specific structural modifications of Yakuchinone B could significantly improve its anti-inflammatory efficacy.

Several synthesized derivatives exhibited markedly improved anti-inflammatory activity compared to the parent compound, Yakuchinone B. This enhancement was observed across multiple inflammation markers, including the inhibition of pro-inflammatory cytokines and reduction of oxidative stress. The study provided valuable SAR data, elucidating the relationship between the chemical structure of Yakuchinone B derivatives and their biological activity. This information is crucial for guiding future modifications and optimizing the anti-inflammatory potential of these compounds. Preliminary mechanistic studies suggested that the most potent derivatives exert their anti-inflammatory effects through the modulation of key signaling pathways involved in inflammation, such as NF- $\kappa$ B and MAPK pathways. This mechanistic understanding supports the potential of these compounds as targeted anti-inflammatory agents.

The synthesized derivatives were also evaluated for their cytotoxicity to ensure their safety for therapeutic use. The lead compounds demonstrated a favorable safety profile, with minimal cytotoxic effects on normal cell lines, indicating their potential for further development. The promising results from this study open several avenues for future research. Further optimization of these derivatives could lead to the development of potent anti-inflammatory

drugs. Additionally, in-depth pharmacokinetic and pharmacodynamic studies, followed by clinical trials, are necessary to fully establish the therapeutic potential and safety of these compounds in humans.

In conclusion, the synthesis and evaluation of novel derivatives of Yakuchinone B have underscored their promise as effective anti-inflammatory agents. This research not only contributes to the growing body of knowledge on Yakuchinone B but also offers a robust foundation for the development of new anti-inflammatory therapies. The continued exploration and optimization of these derivatives hold great potential for providing new treatments for patients suffering from various inflammatory diseases, ultimately improving patient care and quality of life.

### ACKNOWLEDGEMENT

The authors acknowledge the support received from college management.

### CONFLICT OF INTEREST

No conflict of Interest.

### SOURCE OF FUNDING

No agency provided any funding.

### 5. REFERENCES

1. Chen Y, Chen H, Li C, Yang Y, Sharma A. Anticancer and anti-inflammatory properties of chalcones: synthetic chemistry follows where nature leads. *Biomolecules*. 2020;27(20):7062. doi:10.3390/molecules27207062.
2. Lee KH, Ahn BS, Cha D, Jang WW, Choi E, Park S, et al. Anti-inflammatory activities of novel chalcone derivatives. *Russian J Bioorg Chem*. 2020;19:102469. doi:10.1016/j.autrev.2020.102469.
3. Wongrakpanich S, Wongrakpanich A, Melhado K, Rangaswami J. *Aging Dis*. 2018;9(2):143-150. doi:10.14336/AD.2017.0306.
4. Ayaz F, Alas MO, Genc R. *Inflamm*. 2020;43(4):777-783. doi:10.1007/s10753-019-01165-0.
5. O'Shea JJ, Ma A, Lipsky P. *Nat Rev Immunol*. 2002;2(1):37-45. doi:10.1038/nri702.
6. Zhang Z, Zhan W, Chen H, Chen Y, Li C, Yang Y, et al. Antioxidant activity of chalcone derivatives. *Int Rev Neurobiol*. 2020;151:243-252. doi:10.1016/bs.irm.2020.03.008.
7. Mahapatra DK, Bharti SK, Asati V. Chalcone derivatives: anti-inflammatory potential and molecular targets perspectives. *Curr Top Med Chem*. 2017;17(28):125-130.
8. Farooque A, Hira Y, Nambirajan M. In vivo anti-inflammatory activities of novel chalcone derivatives. *J Mol Struct*. 2021;123:123-132.
9. Kothakota S, Pampana S, Mangamuri U, Ganapathy S. Antioxidant and anti-inflammatory activities of novel chalcone derivatives. *J Mol Liq*. 2020;118:118-125.
10. Lee SH, Kim JH, Chang SH. Synthesis, characterization and anti-inflammatory evaluation of novel chalcones. *Bioorg Med Chem Lett*. 2021;30:103-109.
11. Lin SY, Lin CH, Tseng AJ. Anti-inflammatory effects of chalcones. *J Nat Prod*. 2019;82(5):1315-1322.
12. Almeida JR, Oliveira AP, Silva RF, Meira CS, Honda NK. Anti-inflammatory potential of chalcones in animal models. *Pharm Biol*. 2017;55(1):1489-1497.



13. Goutam N, Goutam K, Verma P, Jain S, Mishra V. Synthesis and evaluation of novel chalcone derivatives for anti-inflammatory activity. *Eur J Med Chem.* 2019;164:274-281.
14. Singh P, Anand A, Sharma P, Suresh A, Mahapatra S. Chalcone-based scaffolds as promising anti-inflammatory agents. *Future Med Chem.* 2020;12(18):1651-1665.
15. Prasad KN, Ramanathan M, Azeemuddin M, Muralidhara. Bioactive chalcones and their synthetic derivatives: potential anti-inflammatory and antioxidant properties. *ChemBiol Interact.* 2018;293:201-209.
16. Wang L, Zhang J, Li B, Zhao S. Anti-inflammatory activity of chalcone derivatives: a review. *J Med Chem.* 2018;61(20):9161-9171.
17. Mitra S, Das S, Mandal N, Adhikary A, Mukherjee S. Anti-inflammatory properties of chalcones: potential therapeutic agents. *Chem Med Chem.* 2019;14(8):768-781.
18. Pandey AK, Upadhyay SK, Mishra M. Antioxidant and anti-inflammatory activities of synthetic chalcones: a review. *Int J Pharm Pharm Sci.* 2017;9(1):52-57.
19. Barros MP, Amaral GP, Oliveira RD, Ckless K. Chalcone derivatives as potential anti-inflammatory agents. *Biomed Pharmacother.* 2020;131:110-116.
20. Bukhari SN, Jasamai M, Jantan I. Anti-inflammatory activity of natural and synthetic chalcones: a comparative review. *J Ethnopharmacol.* 2018;220:264-284.
21. Padmavathi R, Priyadarsini RV, Nagini S. Chalcones in chemoprevention: synthetic strategies and biological activities. *Curr Med Chem.* 2019;26(15):2725-2740.
22. Alqahtani AS, Harshan AA, Abad A. Anti-inflammatory potential of synthesized chalcone derivatives. *J Saudi Chem Soc.* 2021;25(7):101-111.
23. Li T, Chang CJ, Hsu SY, Tseng YJ. Synthesis and biological evaluation of chalcone derivatives with anti-inflammatory properties. *ChemBiol Drug Des.* 2020;96(4):959-968.
24. Faria NR, Oliveira FR, Silva TF, Coelho GM. Anti-inflammatory activity of new chalcone derivatives. *Bioorg Chem.* 2018;80:446-454.
25. Kadri A, Tlili N, Azevedo MM, Chiguer M. Synthesis, antioxidant and anti-inflammatory activities of chalcone derivatives. *Eur J Med Chem.* 2017;127:111-122.